

TITLE: THE LASER-FUSION PROGRAM AT LOS ALAMOS

AUTHOR(S): Roger B. Perkins

SUBMITTED TO: Colloquium to be presented at the University of Wisconsin, Madison, Wisconsin, February 17, 1977

By acceptance of this article for publication, the publisher recognizes the Government's (license) rights in any copyright and the Government and its authorized representatives have unrestricted right to reproduce in whole or in part said article under any copyright secured by the publisher.

The Los Alamos Scientific Laboratory requests that the publisher identify this article as work performed under the auspices of the USERDA.



An Affirmative Action/Equal Opportunity Employer

NOTICE
This report was prepared as an account of work sponsored by the United States Government. Neither the United States nor the United States Department of Energy, nor any of their employees, nor any of their contractors, subcontractors, or their employees, makes any warranty, express or implied, or assumes any legal liability or responsibility for the accuracy, completeness or usefulness of any information, apparatus, product or process disclosed, or represents that its use would not infringe privately owned rights.

SM

THE LASER-FUSION PROGRAM AT LOS ALAMOS*

Roger B. Perkins
University of California
Los Alamos Scientific Laboratory
Los Alamos, New Mexico 87545

I. INTRODUCTION TO LASER FUSION

Ever since the realization that the energy production in the sun and the stars is caused by fusion reactions, man has been intrigued with creating energy from such reactions on earth. In the early 1950's, the development of thermonuclear explosives demonstrated the feasibility of producing energy from fusion. In 1955, efforts to develop controlled thermonuclear energy were declassified and an international cooperative program was initiated using magnetic forces to compress and heat thermonuclear material to ignition conditions and to confine the fuel while it burns. In the intervening years, much progress has been made in the magnetic fusion energy program, but production of energy of sufficient magnitude for practical power production has yet to be demonstrated.

Since the late 1960's, a new concept for achieving fusion has been under development--namely using an intense laser pulse to compress and heat a small pellet of fusion fuel to ignition conditions. The fuel, once ignited, would be confined by its own inertia for a short time--long enough to permit a significant portion of it to burn before the heated pellet would fly apart.

* Work performed under the auspices of the U.S. Energy Research and Development Administration.

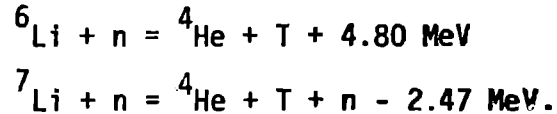
Let us review the fusion reactions which occur at the lowest plasma temperatures (Slide 1). As is well known, energy is given up when the light elements fuse to form heavier elements. As we will see in a minute, the D + T reaction occurs at the lowest energy and yields 17.5 MeV per fusion, 14 MeV to a neutron and 3.5 MeV to an alpha particle. The other reactions require much higher plasma temperatures and hence will not be used for first-generation fusion reactors, if ever. However, they offer potential advantages over the D-T reaction: The D-D reaction eliminates the need to breed T fuel, since D occurs naturally. Further, the lower neutron energy reduces the neutron activation of the reactor structure. The D-³He system is even better since no neutrons are produced and there is a possibility that electricity could be extracted directly from the interaction of these particles with electric and magnetic fields.

Slide 2 shows the fusion cross sections as a function of the particle energy. Clearly the D-T reaction is the most feasible. In a plasma, one has a distribution of velocities which can be characterized by a temperature, generally expressed in electron-volts ($1 \text{ eV} \cong 10^4 \text{ }^\circ\text{K}$). The reaction rate is the product $\langle \sigma v \rangle$ of the D-T reaction cross section and the relative velocity of the D and T nuclei, averaged over a Maxwellian velocity distribution. Slide 3 illustrates the rapid rise in the D-T reaction as a function of temperature, with temperatures greater than about 5 keV required for significant burn rates. If we start with an equal mixture of deuterons and tritons with a total density of $n \text{ atoms/cm}^3$, the thermonuclear power per cm^3 is (Slide 4)

$$p = \left(\frac{n}{2} \right)^2 \langle \sigma v \rangle Q_T$$

where $Q_T = M E_n + E_\alpha = M(14.1 \text{ MeV}) + 3.5 \text{ MeV}$ and M is the blanket energy

multiplication factor. The blanket is designed to contain lithium, which produces tritium by neutron interactions:



In practical designs, about 1.1 T atom can be produced per T atom consumed, and the net energy multiplication factor can be about 1.3 or $Q \sim 22 \text{ MeV}$.

Let us now consider the conditions under which fusion can occur.

Suppose we consider a 1 mg pellet of frozen DT at solid density of 0.2 g/cm^3 (Slide 5). The number density is $5 \times 10^{22} \text{ atoms/cm}^3$ so 1 mg contains 2.4×10^{20} atoms and is a sphere 1 mm in radius. If we heat the pellet to $10^8 \text{ }^\circ\text{K}$ or 8.6 keV essentially instantaneously, we must invest $3 nkT = 1 \times 10^6 \text{ J}$. The inertial confinement time $\tau_e = \frac{R}{4C_s}$, that is, the radius divided by sound speed in the hot plasma (the factor of 4 arises from the average mass in the sphere during its disassembly). The sound speed or thermal velocity of the ions is 10^8 cm/s at this temperature, so the disassembly time $\tau_e \sim 2.5 \times 10^{-10} \text{ s}$. The reaction time $\tau_r = \frac{1}{n \langle \sigma v \rangle} \approx 4 \times 10^{-7} \text{ s}$ under these same conditions. The fractional burnup of the pellet is approximately given by

$$f \sim \frac{\tau_e}{\tau_r} = \frac{\langle \sigma v \rangle}{4m_i C_s} \rho R = \frac{1}{1600}$$

in this case. The energy out, assuming $Q = 17.5 \text{ MeV}$, is therefore $E_{\text{out}} = 326 \text{ MJ/mg} \times 1 \text{ mg} \times \frac{1}{1600} = 0.2 \text{ MJ}$, only 1/5 of what we had to invest to heat the pellet.

Clearly, we have to do better. How is this accomplished? Notice that the fractional burnup is proportional the product ρR , the other factors being only a function of the temperature at which the reaction occurs. The product

$\rho R \propto \frac{1}{R^2}$, so if we can raise the density of the pellet, we will increase the fraction burned even though the disassembly proceeds more quickly. Suppose we are able to compress the pellet radius in our example by a factor of 10 to 0.1 mm. Then the density would increase 1000 fold and (Slide 5 overlay)

$$\begin{aligned}\tau_e &\sim 2.5 \times 10^{-11} \text{ s} \\ \tau_r &\sim 4 \times 10^{-10} \text{ s}\end{aligned}$$

and $f \sim 0.06$.

In this case $E_0 = 20 \text{ MJ}$, so we have obtained 20X the incident power. This is still not much gain, for we will have to overcome the inefficiencies of converting the heat to electricity (.35), of producing the laser energy from electricity (.05), and finally losses due to lack of perfect absorption of the laser light by the pellet (.3). The product of all three factors is about 1/200 so we still miss breakeven by a factor of 10. However, at these conditions, the range of the alpha particles is only 0.3 g/cm^2 , whereas the absorption length in one pellet radius is $\rho R = 2 \text{ g/cm}^2$. Twenty percent of the nuclear energy is redeposited in the pellet, providing a bootstrap mechanism which reduces the incident laser requirements. In fact, one need only ignite the center of the pellet to create a propagating burn wave from the alpha particles which then can ignite and burn a substantial portion of the pellet.

Finally, are there tremendous density increases even possible? Calculations indicate that a pressure of at least 10^{12} atmospheres is required to achieve 10,000 fold compression, the level believed necessary to achieve adequate gains to overcome the inefficiencies and produce net power. Surprisingly, the energy required for this compression is only 1% of that needed to heat the DT pellet to ignition temperature, so all we need is a mechanism.

In laser-driven fusion, the laser light is focused symmetrically on the spherical pellet. The light is absorbed in the low density atmosphere which quickly forms by electron-ion interactions or by plasma instabilities, creating hot electrons with energies measured in thousands of volts. The absorption occurs predominately in the critical-density region, where the index of refraction becomes imaginary. ($n = 10^{21}/\lambda^2$ where λ is the light wavelength in μm). (Slide 6). The hot electrons produced by the laser-plasma interaction diffuse around the pellet and heat its surface, causing particles to ablate, which creates a spherical rocket effect which causes an implosion of the pellet.

To minimize the total energy required, the compression must be done carefully by tailoring the laser energy with time, and one also must avoid preheating the core of the pellet. Many of the current experimental and theoretical studies are addressing the detailed understanding of these processes, and I will elaborate on some of these topics later. Further, unless the implosion is symmetrical, both in the initial stage and late in the process, the yield will be significantly degraded. Thus, the laser illumination must be very smooth, and one must avoid hydrodynamic instabilities by careful design.

Sophisticated computer programs have been developed to study the laser-driven implosions and resulting explosions. It is now generally agreed that a laser delivering about 100,000 joules in about 1 ns will be required for scientific breakeven, where the thermonuclear yield equals the laser light absorbed by the pellet. Net energy production is expected to require in excess of 1 MJ from the laser per microexplosion.

II. LASER CHOICES

What is the status of high power, short pulse lasers? (Slide 7). Early in the program, Nd:glass lasers were quickly adopted for experiments, since they were capable of quite high power and energy levels and could be produced off the shelf from a number of manufacturers. At LLL, these large laser systems based on Nd:glass have been developed by increasing the power outputs and by combining large numbers of beams. John Holzlrichter has given you a colloquium during the past year which described the LLL systems. They hope to attain power levels of 25 TW with the Shiva laser now near completion. However, the average power output of a single beam and the repetition rate of the Nd:glass laser is limited due to the very slow cooling capability of a solid like glass. Further, the efficiency is very low, being about 0.1% in current systems. Thus, present-day Nd:glass lasers have no chance of being incorporated into a laser-fusion reactor concept. /

Los Alamos adopted a different approach by developing the CO₂ laser. This laser is based on exciting a gas medium composed of nitrogen and carbon dioxide, and the efficiencies turn out to be several percent. Further, since the laser medium is a gas, it is in principle capable of high repetition rates and high power output if one uses a flowing system. The main drawback of the laser is its wavelength, 10.6 μm, ten times that of Nd:glass and in the far infrared. This wavelength required use of special window materials and was thought to be disadvantageous for pellet implosion about which I will speak later.

A search has been underway for a so-called Brand X laser, a gas laser of visible or near-visible wavelength but with high efficiency. A number of candidates are being explored throughout the world, but to date, none seems to have the desired set of features.

Alternate driver schemes are being explored. Electron-beam accelerators offer much higher efficiency, but suffer from the difficulty of transporting the very high current and current density but relatively low voltage beams to the pellet target. Thus, if the scheme can be made to work, one will have to solve the standoff problem, i.e., avoiding destruction of the machine by the fusion output.

Recently, the use of very heavy ions has been proposed. Multi-ampere beams of multi-GeV uranium ions appear to be best. But the difficulties and high potential cost of this approach require further consideration.

III. CO₂ LASERS

I will now describe the CO₂ laser development program at LASL and the facilities that are being constructed and used. But first, I will briefly describe how these devices work:

The CO₂ laser, as with any laser, requires a population inversion between the two atomic or molecular states involved in the optical transition of interest. The kinetics are quite complicated in this system, so I won't try to explain them in any detail. The excitation is provided by electrical power, which imparts kinetic energy to electrons which in turn excite predominantly the first vibrational state of N₂. This level is nearly coincident in energy with the upper level of the 10.6 μm transition in CO₂, and the excitation is relatively quickly shared between the N₂ and CO₂ by molecular collisions.

To obtain the very short, single pulses needed for laser-fusion studies, one must use a system similar to that shown on the next slide (Slide 8). At the front end one has an oscillator which is capable of generating a train of short 10.6 μm pulses. One of these, typically 1 ns long, is switched out through an electro-optical shutter. Its power level can be very small, but it must be completely free from pre-pulses. Then the pulse is sent to a series of amplifiers, which consist of CO₂-N₂ gain media pumped to an inversion level slightly below that which would lead to spontaneous light output. When the trigger pulse from the oscillator propagates through the amplifiers, stimulated emission occurs and the pulse power increases.

A number of conflicting technical and physical constraints affect the design of the high power amplifiers. First, to get short intense pulses, one must use pressures of about 3 atmospheres.

Second, the laser medium must be preionized with electrons during the main discharge, and the electron kinetic energy requirements increase with increasing pressure and aperture. Finally, the intensity in the pulse must be limited to less than 2 J/cm^2 to avoid damage to the exit window of the laser. The window must be transparent to $10.6 \mu\text{m}$ light and the best choice is NaCl. However, salt is not very strong and is available only up to diameters of about a foot, thus placing a limit on the aperture size and a further limit on the pressure in the pumping media.

These various constraints, together with others not discussed, have led to a basic amplifier design shown in the next slide (9). The 200 keV electrons are generated in a vacuum diode, penetrate a Ti window into the 3 atmosphere lasing medium, providing ionization for a high intensity electrical discharge (Slide 9a as backup). The medium is pumped for several microseconds before the laser pulse to be amplified arrives. The next slide (10) shows the actual hardware used in our dual beam module. The design point of this module is 1250 joules per beam with a 1 ns pulse length. We have observed 850 joules output from each beam without a target in place, but have been limited to beam energies of about 350 joules with targets due to a decreased oscillation threshold arising from target reflections. In December, experiments started using both beams simultaneously. A number of improvements are planned which will increase the output energy and decrease the pulse length, both improving the output power.

With all laser systems, one must worry about retro-pulses due to target reflections which can send massive pulses back up the laser and destroy sensitive components. In glass laser systems, with relatively small aperture, Faraday rotators can be employed after a polarizer to eliminate retro-pulses. Research continues on large aperture rotators suitable for our CO₂ systems, but a simpler scheme has been found. If a focus or near focus is formed in the final amplifier near its input, retro-pulses which become amplified to dangerous levels will simply cause optical breakdown near the focus in the laser medium, and the resultant absorption and refraction fraction protects the upstream components.

The next slide (11) shows the sequence of CO₂ lasers which are under construction at Los Alamos, for laser-fusion experiments. The SBS has been in use for several years for laser-target interaction studies. The TBS uses the dual beam module shown in the previous slide, which is a prototype for the EBS, a laser which will provide 10⁴ joules when operational next year. Finally, the HEGLF is being designed to provide 10⁵ joules which is the energy level believed needed to reach scientific breakeven.

The next slide (12) shows a drawing of the EBS. (point out features). The next slide (13) shows details of the 4-dual beam modules which will provide 8 beams to the target chamber at the center. Note that the optics consist entirely of copper mirrors which are highly reflective for the 10 μm light. Finally, the target chamber is shown in the next slide (14). (Discuss) Operation and alignment of the optics will be controlled by a computer system.

The HEGLF again is based on the concept of the dual beam module. In this design, the final power amplifier (Slide 15) uses a common central electron gun with an annular arrangement of a dozen laser chambers. The segmentation of the beam into 12 parts is dictated by the size limits on the salt windows

mentioned earlier. Six of these amplifiers will be aimed at a single target as shown in the next slide (16). The facility was fully authorized a few months ago at a cost of \$55M. It is scheduled for completion in 1981.

In addition to the usual problems associated with a construction project of this magnitude, a number of special problems deserve mention. The optical system must focus 6 beams simultaneously (within a few picoseconds) onto the target with a 400 μm focal spot size. This requires essentially perfect optics throughout the system, for a perfect system, where no errors in pointing or surface finish would exist, would still have a finite spot size of about 300 μm due to diffraction effects. The quantity of mirrors required, if hand polished, would require the full output of world's mirror and lens makers for many years and the quality would be inadequate. Therefore, in conjunction with the Oak Ridge Y-12 plant, we have had to develop diamond-point micromachining and optical inspection techniques to machine copper mirrors to an accuracy of about 1 μm or one-tenth of a wavelength. The process is fast and cheap and requires no hand finishing (Slide 17).

Another problem is that of electromagnetic interference. With the intense electrical currents and voltages which provide the excitation of the lasers microseconds before the laser pulse hits the target, plus the strong electromagnetic and nuclear signals which will occur when 100 kJ is converted to nuclear output, target diagnostic signals must be very carefully shielded from this noise. In the HEGLF, we have decided that only fiber optical cables will be sufficiently insensitive to pickup. Therefore, all control and experimental wiring will be contained in well-shielded boxes, interconnected via fiber optics. Microprocessors will be used for the interface between each end of each fiber to the electronic actuators or transducers. The entire complex will be controlled from a central location with a well-shielded computer system.

The HEGLF will be our major facility when completed in 1981. The research program will include basic experiments and military applications, but the main thrust will be to achieve scientific breakeven on suitable targets, where the output power equals or exceeds the input laser power. The facility is being designed to handle 200 shots per year with adequate shielding for the up to 5×10^{17} neutrons per microexplosion. Once scientific breakeven is achieved, studies will continue to reach higher gains with improved designs, and to simplify pellet designs to permit automation of fabrication and, hence, a lowering of their cost.

Follow-ons to HEGLF are now being studied, since it may turn out that no better laser is invented and developed. CO_2 lasers are scalable to higher powers and improved efficiencies should be achievable with further engineering development. In particular, efficiencies approaching 30% may be possible by multiple pulse extraction. Further, being a gas laser, high repetition rates are also quite feasible and we are working closely with industry to be able to move into a flowing gas laser concept if appropriate. An experimental laser-fusion reactor would almost certainly not be built at a national lab such as Los Alamos, but we would like to exploit HEGLF and its possible follow-ons to a maximum possible extent to reduce total costs and time delays in achieving commercial laser-fusion power, assuming it is possible.

IV. RECENT TARGET INTERACTION EXPERIMENTS

I can only sketch briefly some of the target experiments that are in progress. Many of these experiments have been performed on simple slab targets, but others have required use of low mass, symmetric spherical targets. With laser powers currently available, spherical gas targets with a diameter of approximately 100 μm (a tenth of a mm) are required. These are most conveniently made by using tiny hollow spheres of glass into which DT can be diffused at high temperature to produce stable targets which contain up to 100 atmospheres at room temperature with gas lifetime measured in months. The glass spheres or microballoons are made commercially but must be rigorously selected to find the approximately one in a million that has a uniform wall and symmetric shape.

The next slide (18) shows an example of a small gas-filled microballoon of 75 μm diameter. A more typical target used with the two-beam laser is the ball-and-disk target shown on the next slide (19). The disk intercepts part of the laser energy and provides more uniform heating of the sphere.

Experiments are underway at the present time with the SBS and TBS CO_2 lasers and also a 200 joule Nd:glass two-beam system, the latter facility being useful for comparing laser-target interactions at the 1.06 μm wavelength. A variety of techniques are employed for experiments ranging from photographic films, track detectors, and neutron activation detectors to very sophisticated x-ray streak cameras, x-ray microscopes, and multiple-frequency interferometers. (Slide 20).

Experiments are compared with theoretical calculations to both calibrate the codes, and to gain confidence of the predictive capacity. Since the codes are only one- and two-dimensional, the calculations can only approximate real three-dimensional objects interacting with real laser beams. Our main analytical

tool is the LASNEX code originally developed at Lawrence Livermore Laboratory, to which we now contribute improvements which are shared by both laboratories.

One of our main experimental and theoretical efforts during the past year has been the elucidation of the wavelength scaling question. That is, the question of whether the long 10.6 μm CO_2 wavelength would be appropriate for laser-fusion (Slide 21). First, let us review the objections to long wavelengths. This slide simply shows a schematic of the plasma blowoff cloud from a solid target with a beam incident from the right. The laser light does not penetrate beyond the so-called critical density, the point where the index of refraction goes through zero, corresponding to the point where the local electron plasma frequency equals the incident laser frequency. Since the critical density $n_c = \frac{10^{21}/\text{cm}^3}{\lambda^2(\mu\text{m})}$, the 10.6 μm CO_2 light penetrates only to a density 100 times lower than the Nd laser light. For a hydrodynamically expanding plasma, the CO_2 light is absorbed at a much larger radius, and because of the low density, the energy deposited per particle is much higher.

It was believed that CO_2 laser light would therefore generate very energetic "suprathermal" electrons in this absorption region, and these electrons could cause severe preheating of the target core because of their long range. Achieving isentropic compression of the preheated fuel is more difficult and energy consuming.

A number of methods of determining the suprathermal electron energies have been devised. One method is to look at the maximum ion energies, assuming that the ion velocities will be related to the suprathermal electron energies present in the target. The result was that at comparable flux densities of about 10^{15} W/cm^2 , the maximum ion velocities observed with Nd and CO_2 lasers were about the same.

Similarly, high energy x-ray spectra measurements from both Nd and CO₂ laser experiments also indicated similar hot electron temperatures of about 15 KeV. Also, the energy spectra of electrons which leave the target are similar for both wavelengths, though the interpretation of the spectra is complicated by the fact that the detected electrons must cross large time-dependent potentials.

We have realized in the past year that the ponderomotive force (the force due to the pressure exerted by the laser light at high intensities) has been neglected in the wavelength argument (Slide 22). Consider the ratio of the radiation pressure to the plasma pressure at the critical density. At 10^{15} W/cm², assuming a plasma temperature of 1 keV, the ratio is much greater than one for CO₂ laser light and approaching one even for Nd. In this region, we would expect the plasma profile to be strongly distorted by the laser, especially in the vicinity of the critical density. In particular, for the CO₂ experiments we might expect the laser ponderomotive force to drive up a very large density step whose upper density might be comparable to the Nd critical density. This could explain the similarity in results between the two wavelengths.

More recently, we have combined all data that we could find on hot electron temperatures and plotted it versus P_L (Slide 23). We note that all the points seem to lie on a single curve for a single wavelength. Further, if we plot the data as a function of $P_L \lambda^2$, (Slide 24), the data coalesces to a single curve, characterized by three regions. In the upper region, where strong profile modification effects are likely due to the high ratio of ponderomotive pressure to plasma pressure, the slope of the curve is 0.25, implying that the hot electron temperature is scaling as the square root of the wavelength. Thus, it appears that CO₂ radiation may be nearly as satisfactory as Nd:glass radiation.

In both cases, we will have to worry about fast electron preheat in target designs. One scheme which we are considering is called vacuum insulation. (Slide 25). The leakage of a few electrons causes a buildup of an electrostatic potential which repels the bulk of the remaining hot electrons, which oscillate through the outer shell gradually losing energy by collisions. Eventually, after a fraction of a nanosecond, the vacuum is shorted out by plasma flowing across it, but we believe that the preheat will have been avoided at the crucial time.

Finally, we have incorporated the vacuum insulation feature into a HEGLF target design (Slide 26), which we believe will reach scientific breakeven at an input energy of about 30 kJ. Such calculations are subject to many approximations, so we will have to wait for HEGLF to test it.

V. CONCEPTUAL POWER PLANTS

I now wish to discuss commercial applications of laser fusion, assuming we have success in burning pellets at significant gain. Figure 27 shows a simplified flow diagram for a laser-fusion electric generating station. Electrical power drives the laser, whose light is transported to the fuel pellet in a suitable reactor cavity. The neutrons deposit their energy in a lithium blanket which serves the dual function of breeding tritium and transferring the heat to a steam turbine. The turbine drives a generator, yielding electrical power to the grid and to the laser system. The tritium produced in the blanket is separated, combined with deuterium, and fabricated into suitable fuel pellets.

What are the energy flow considerations in such a process? Figure 28 shows a block diagram. η_I is the efficiency of the injector or laser. γ is the net output energy of the pellet compared to the input laser power. It is the product of the pellet gain and the fractional absorption of the laser light by the pellet. η_T is the efficiency at which heat is converted to electricity. ϵ is the circulating power, which practically must be kept below about 0.3 to keep the capital costs of the plant within bounds. Using the estimates shown in the figure, a pellet gain of about 600 is required, which will require central ignition and propagating burn of the pellet.

Understanding of the physics of laser-induced fusion must await the availability of higher power lasers. However, it is believed that the pellets will involve DT fuel either as a cryogenic solid or as high pressure gas in solid shells. The output of the burning pellet will appear as neutrons for about 75% of the energy, up to 5% as photons, and the remaining 20% or so will be absorbed by the pellet. Some fraction of the absorbed energy will appear at the reactor cavity first wall as debris from the pellet materials.

The main engineering problem of laser-fusion reactors is to contain the energy of the pellet explosions by a suitable cavity for some 10^9 to 10^{10} pulses over the reactor lifetime. A typical pellet energy yield is 100 MJ, corresponding in energy to roughly 20 kg of high explosive. A repetition rate of 1 to 10 per second is believed desirable.

A number of laser-fusion reactor concepts have been investigated. The wetted-wall concept is shown in the next slide (29).

The reaction chamber is spherical and is surrounded by a lithium blanket. The cavity wall is made of a porous refractory metal through which coolant lithium flows to form a protective coating on the inner surface. Part of this layer is ablated by each pellet microexplosion and the evaporated lithium is exhausted through a supersonic nozzle into a condenser. For a 100 MJ microexplosion, a 3.4 m minimum diameter chamber is required to avoid overheating of the wall by x-ray energy deposition. At this diameter, a 0.1-mm-thick film of lithium would be vaporized by each microexplosion and such a layer could be restored in a fraction of a second by inward flow.

A crude vacuum must be maintained ($\sim 10^{17}$ atoms/cm³ or 1/100th of an atmosphere) to avoid optical breakdown by the incident laser light. Analyses of the blowdown phenomena indicate about a second is required to restore the cavity to this condition after each microexplosion. Therefore, a maximum repetition of 1 per second or about 100 MW would be appropriate for a wetted wall reactor concept.

In this design, a tube would be used to inject pellets. Eight laser-beam transport tubes would be used to provide reasonably symmetric illumination.

Blanket structures have not been designed in detail, but acceptable breeding ratios can be achieved. 100 MJ microexplosions can be contained without exceeding fatigue limits using niobium, molybdenum, or stainless steel at temperatures up to 1000 K.

An alternative concept uses a solenoidal magnetic field to protect the cavity walls from energy deposition and erosion. This scheme is shown on the next slide (30). The central portion of the cavity and its blanket is within the solenoid. Alpha and other ionized particles in the pellet debris are diverted by the magnetic field to conical energy sinks in the ends of the cylindrical cavity.

Studies have been made of the behavior of the cavity. The alphas act as single particles, going into gyro-orbits of about 1 m radius for $B_z = 2000$ gauss, and spiraling out the ends to the energy sinks. The much slower debris acts collectively; it excludes and then compresses the B field between the plasma and the cavity wall, with pressure balance occurring at a 2 m radius. After several bounces against the field, the plasma expands toward the energy-sink regions.

A cavity radius of 5 m was chosen to avoid excessive x-ray heating of the inner wall of the blanket. Carbon appears to be a satisfactory wall material, and a refractory metal carbide is used for the energy-sinks. Again liquid lithium is used for tritium breeding and heat exchange. The energy-sinks subtend only 10% of the solid angle and need not be cooled by lithium and be part of the tritium breeding region.

The potential advantage of this concept is the relatively convenient replaceability of the energy sinks which will bear the brunt of the damage from pellet radiations. Also, higher repetition rates should be possible. Further, the magnetic field will shield the last optical elements from charged particle damage. Finally, the tailoring of the fringing fields at the energy-sink region will permit a lowering of energy density in space and time which should reduce temperature swings and deterioration of the surfaces.

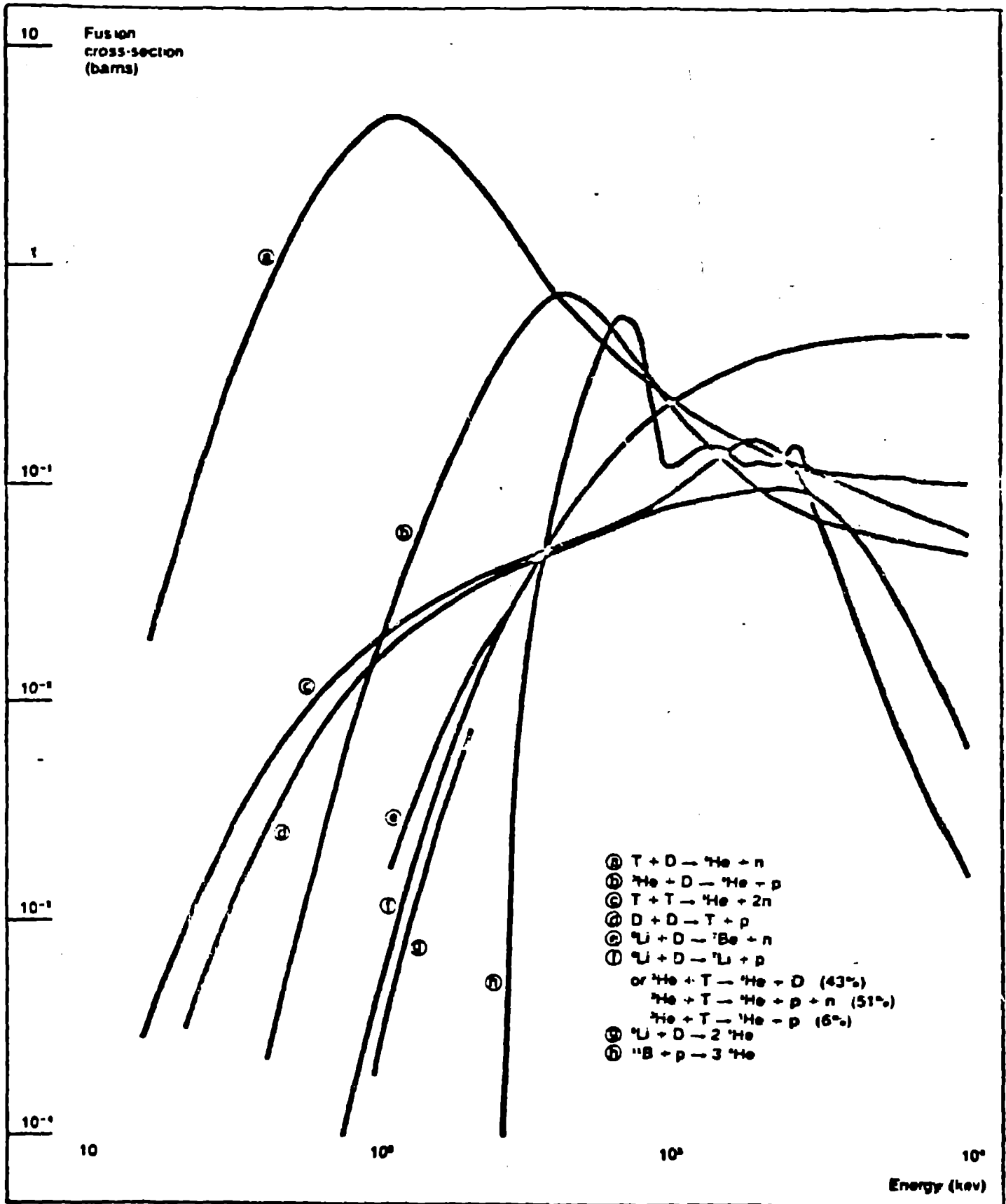
Finally, laser-fusion hybrid concepts have been considered, where fissionable material is incorporated in the blanket. Two major features have emerged from these considerations: (1) hybrids have the potential to produce fissile fuel and power with an order of magnitude lower laser/pellet performance than required for pure laser fusion, and (2) the hybrids produce 10 times more fissile fuel per unit of thermal energy generated than fission breeder reactors. So such hybrid reactors may provide an intermediate path if the difficulties of pure laser fusion are too great.

A schematic view of an electric generating station is shown in the next slide (31), based on the magnetically protected concept. Four reactors with a thermal power output of 1250 MW each are included. Hot-cells are provided to service the energy-sink cones. Separate heat-exchanger and lithium-tritium separator systems are provided for each reactor. The laser power supplies are on the 2nd floor and the 16 CO₂ laser power amplifiers are on the 3rd. Only 8 lasers are used at once, the light being directed to the cavities successively by a rotating mirror system.

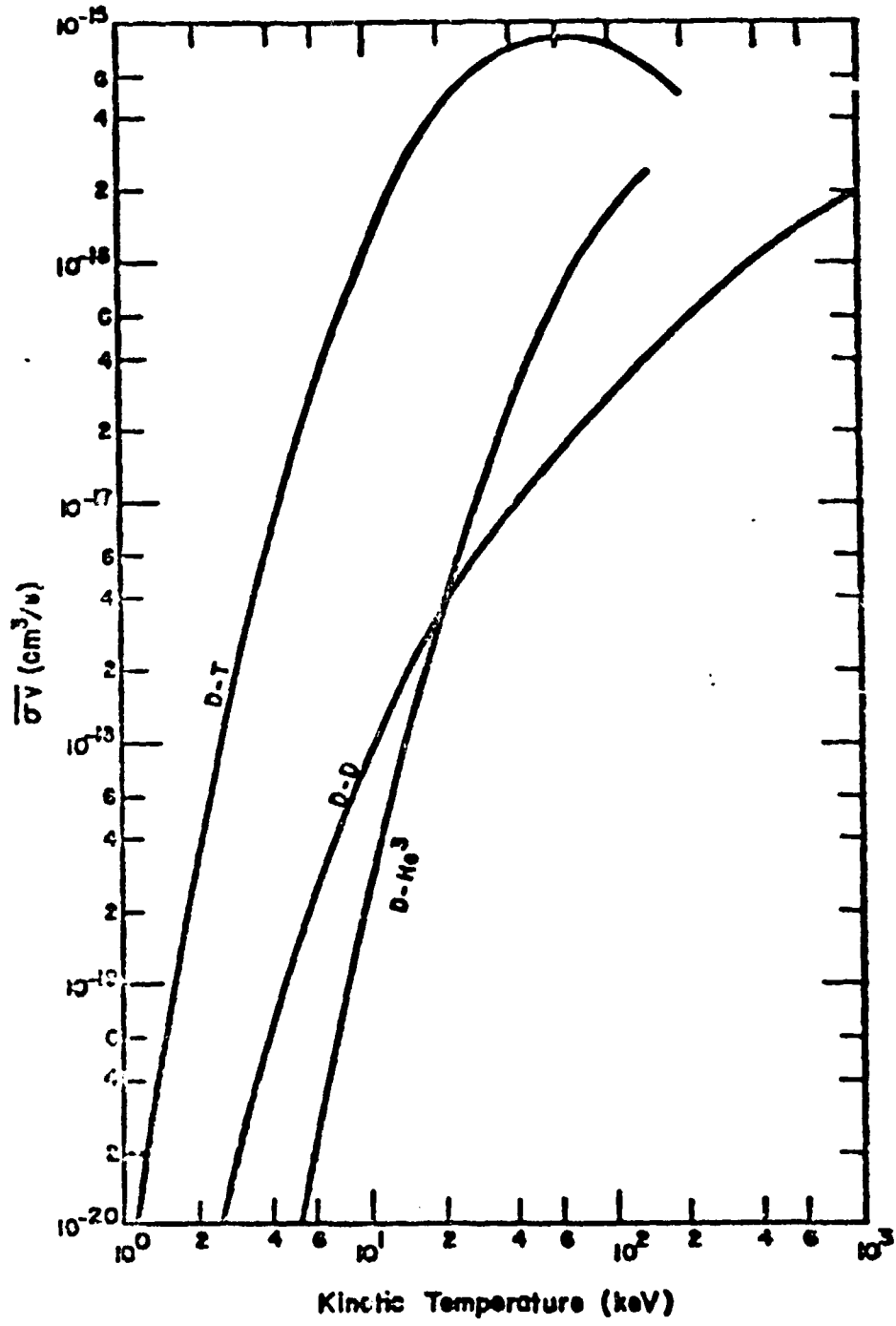
A schedule has been developed for commercial use of laser fusion. (Slide (32)). It projects operating of an EPR in the 1990's and operation of a demonstration reactor in 2000, leading to commercialization after the year 2000. In spite of this overly optimistic schedule, the promise of laser fusion appears to be sufficiently great that a vigorous program is well justified. The problems encompass a broad range of physical and technical areas and are an exciting challenge to everyone involved.

NUCLEAR FUSION REACTIONS

REACTION	TOTAL ENERGY (MEV)	CHARGED PARTICLES (MEV)
$D + T \longrightarrow {}^4\text{He}(3.52 \text{ MeV}) + n(14.06 \text{ MeV})$	17.58	3.52
$D + D \longrightarrow {}^3\text{He}(0.82 \text{ MeV}) + n(2.45 \text{ MeV})$	3.27	0.82
$D + D \longrightarrow T(1.01 \text{ MeV}) + p(3.03 \text{ MeV})$	4.04	4.04
$D + {}^3\text{He} \longrightarrow {}^4\text{He}(3.67 \text{ MeV}) + p(14.67 \text{ MeV})$	18.34	18.34
$T + T \longrightarrow {}^4\text{He} + n + n$	11.32	---



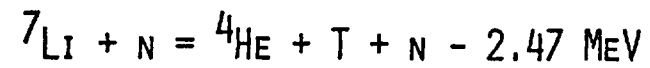
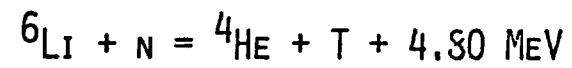
SLIDE 2



SLIDE 3

$$P = \left(\frac{N}{2}\right)^2 \langle \sigma v \rangle Q_T$$

$$Q_T = M E_N + E_\alpha = M(14.1 \text{ MeV}) + 3.5 \text{ MeV}$$



SLIDE 4

PELLET BURN CONSIDERATIONS

$$1 \text{ MG DT} = 2.4 \times 10^{20} \text{ ATOMS IN SPHERE OF 1 MM RADIUS}$$

$$\left[\begin{array}{l} \rho = 0.2 \text{ g/cm}^3 \\ n = 5 \times 10^{22} / \text{cm}^3 \end{array} \right]$$

$$10^8 \text{ K} = 8.6 \text{ KEV REQUIRES } 3 \text{ NKT OR } 10^6 \text{ JOULES}$$

$$\tau_E = R/4C_S \text{ SEC} \quad 2.5 \times 10^{-10}$$

$$C_S \sim 10^8 \text{ CM/SEC}$$

$$\tau_R = 1/N \langle \sigma v \rangle \text{ SEC} \quad 4 \times 10^{-7}$$

$$f \sim \frac{\tau_E}{\tau_R} = \frac{\langle \sigma v \rangle \rho R}{4 n C_S} \quad 1/1600$$

$$E_{\text{OUT}} \quad 0.2 \text{ MJ}$$

ρ_{MAX} (G/CM³)

0.2

200

2.5×10^{-11}

4×10^{-10}

1/16

20 MJ

SLIDE 5 (OVERLAY)

Hot
Expanding
Plasma

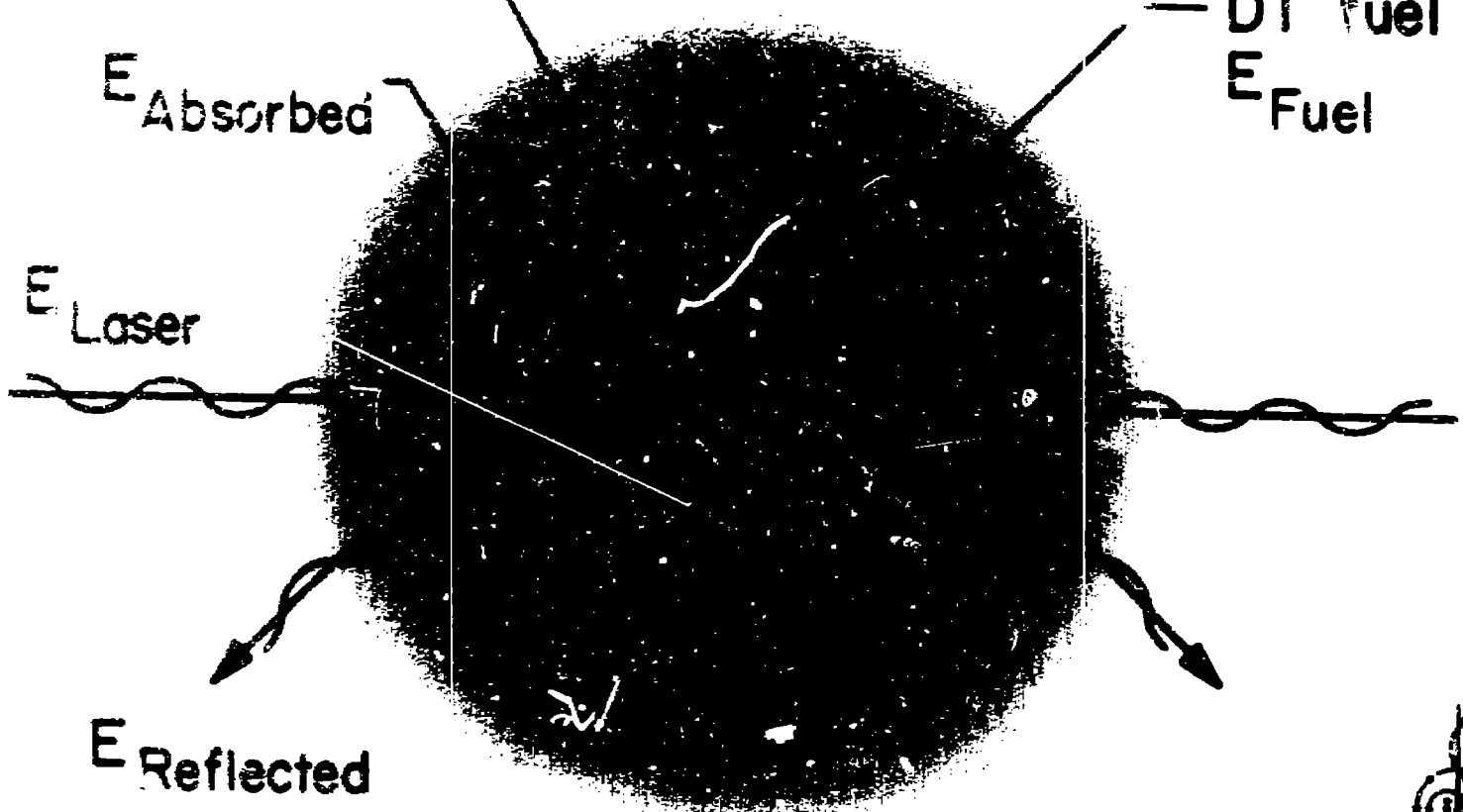
Imploding
DT fuel

E_{Absorbed}

E_{Fuel}

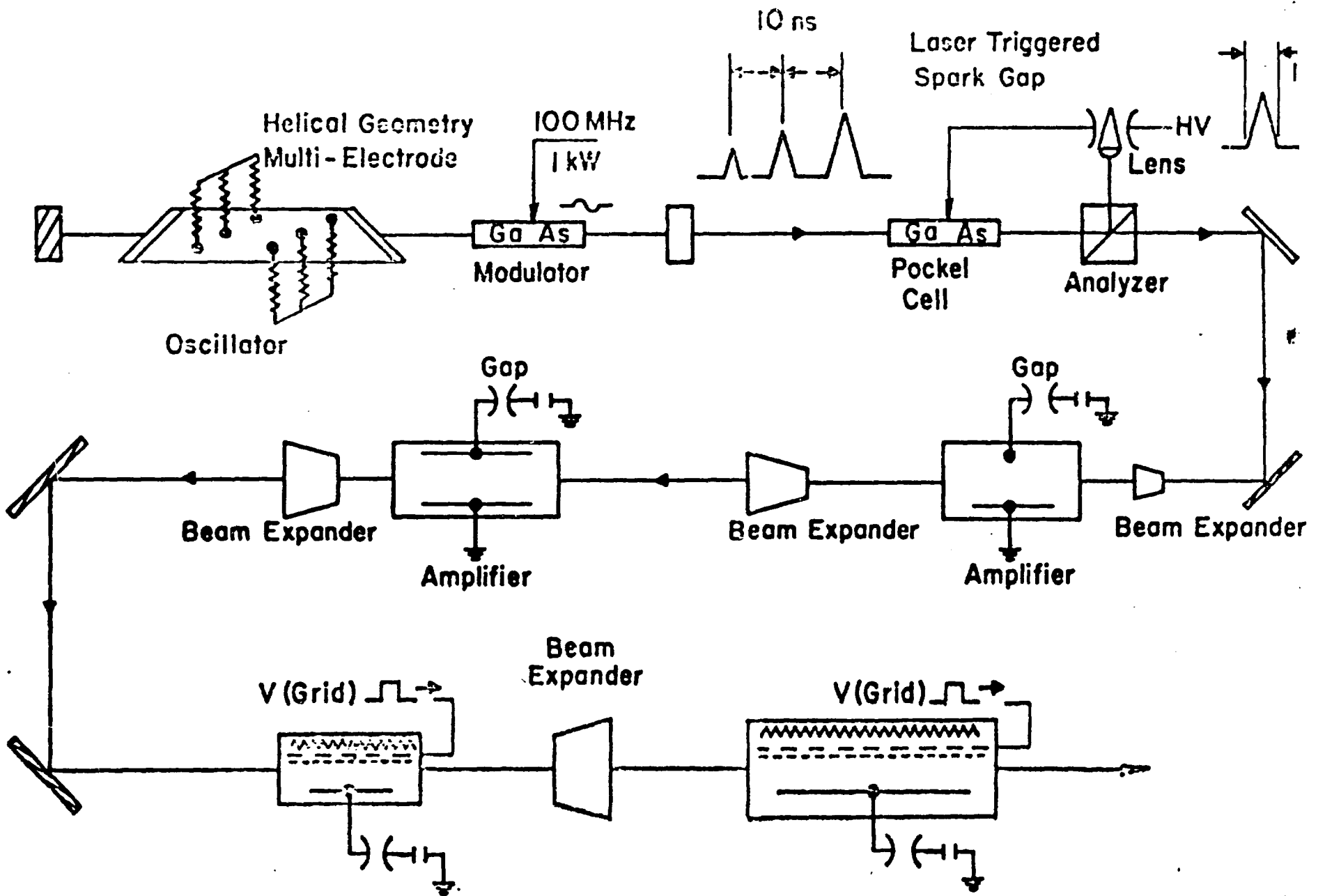
E_{Laser}

$E_{\text{Reflected}}$

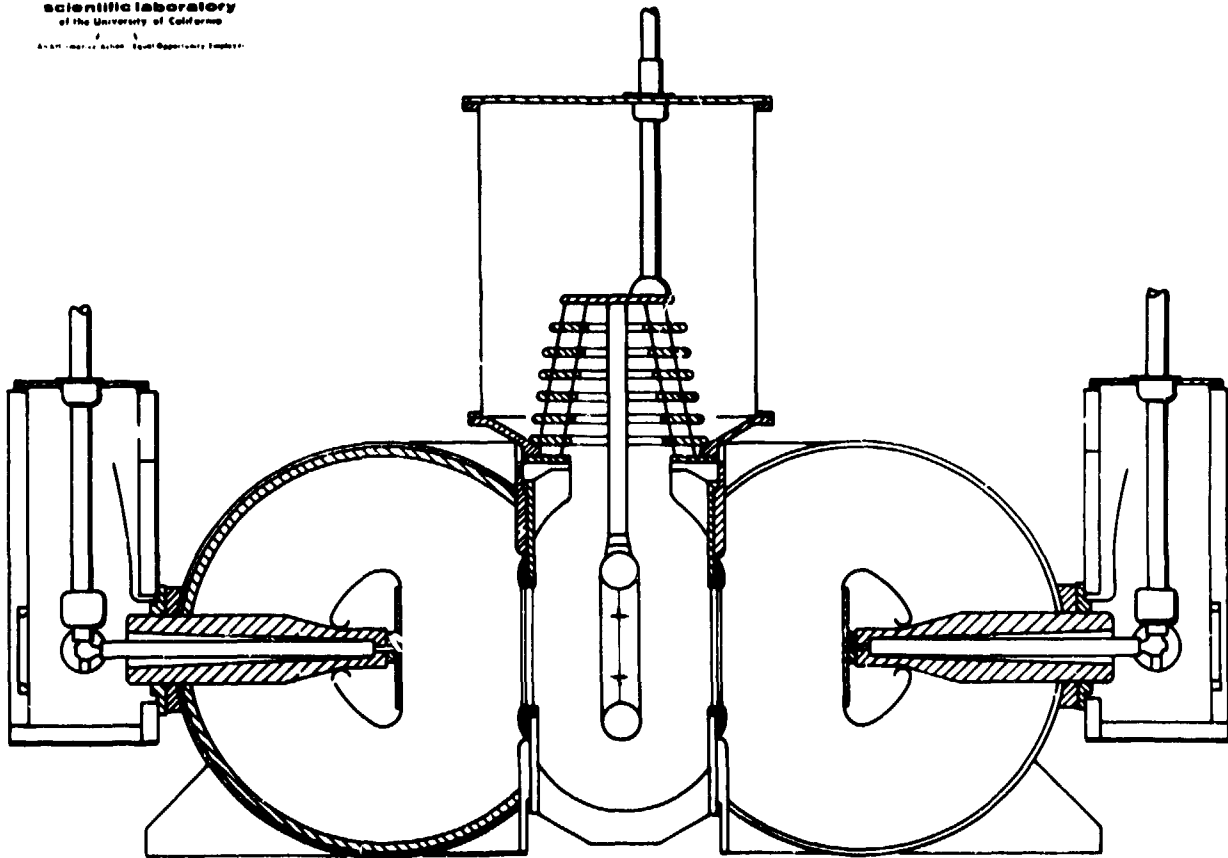


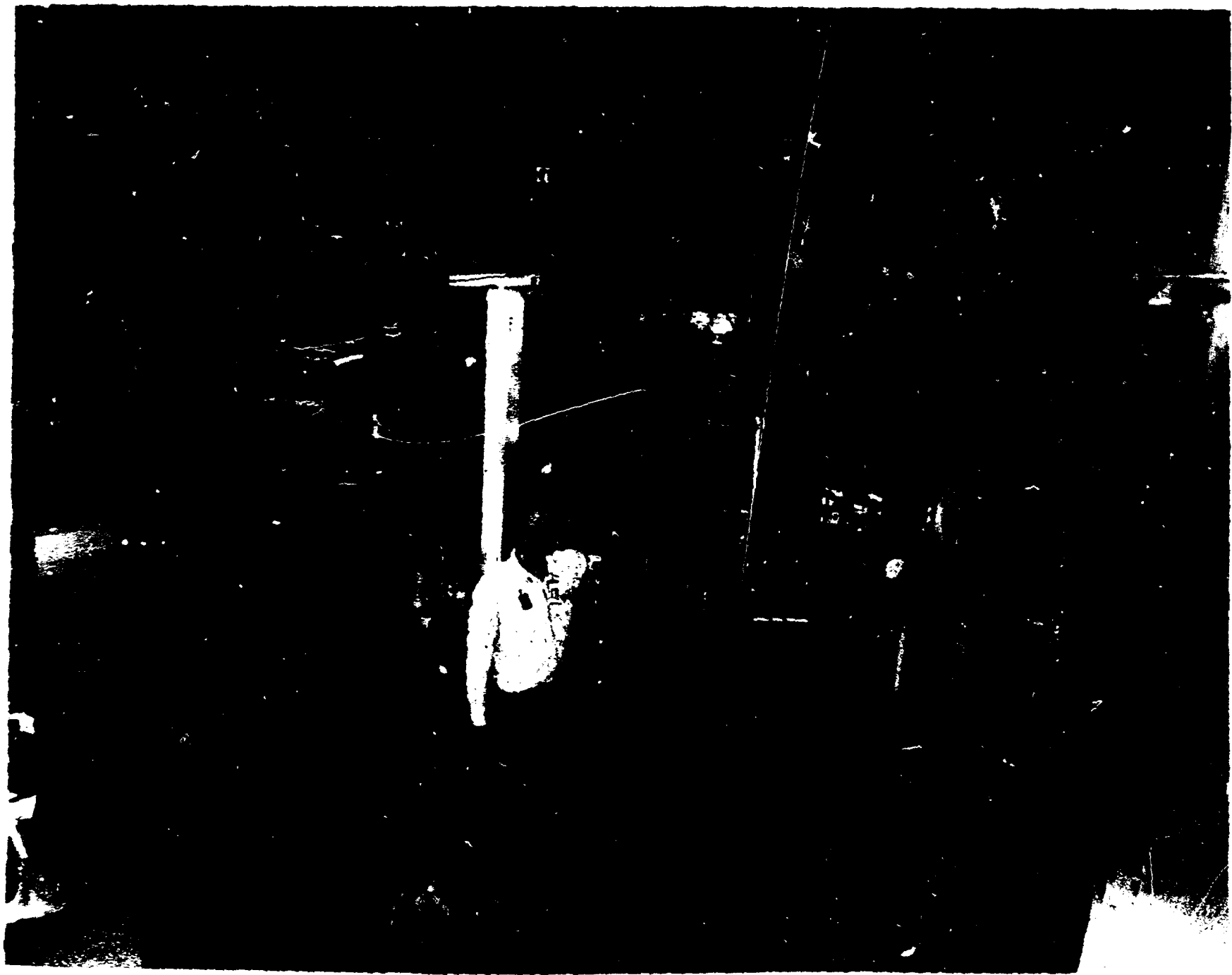
	<u>PRESENT EXPECTATIONS</u>		<u>PROJECTED NEEDS</u>
	Nd:GLASS	CO ₂	BRAND X
λ	1.06 μM	10.6 μM	?
EFFICIENCY	0.1 - 0.2%	5 - 7%	5 - 20%
PEAK POWER	200 - 300 TW	100 - 200 TW	1000 - 10,000 TW
REP. RATE	LOW	1 - 10 Hz	1 - 10 Hz

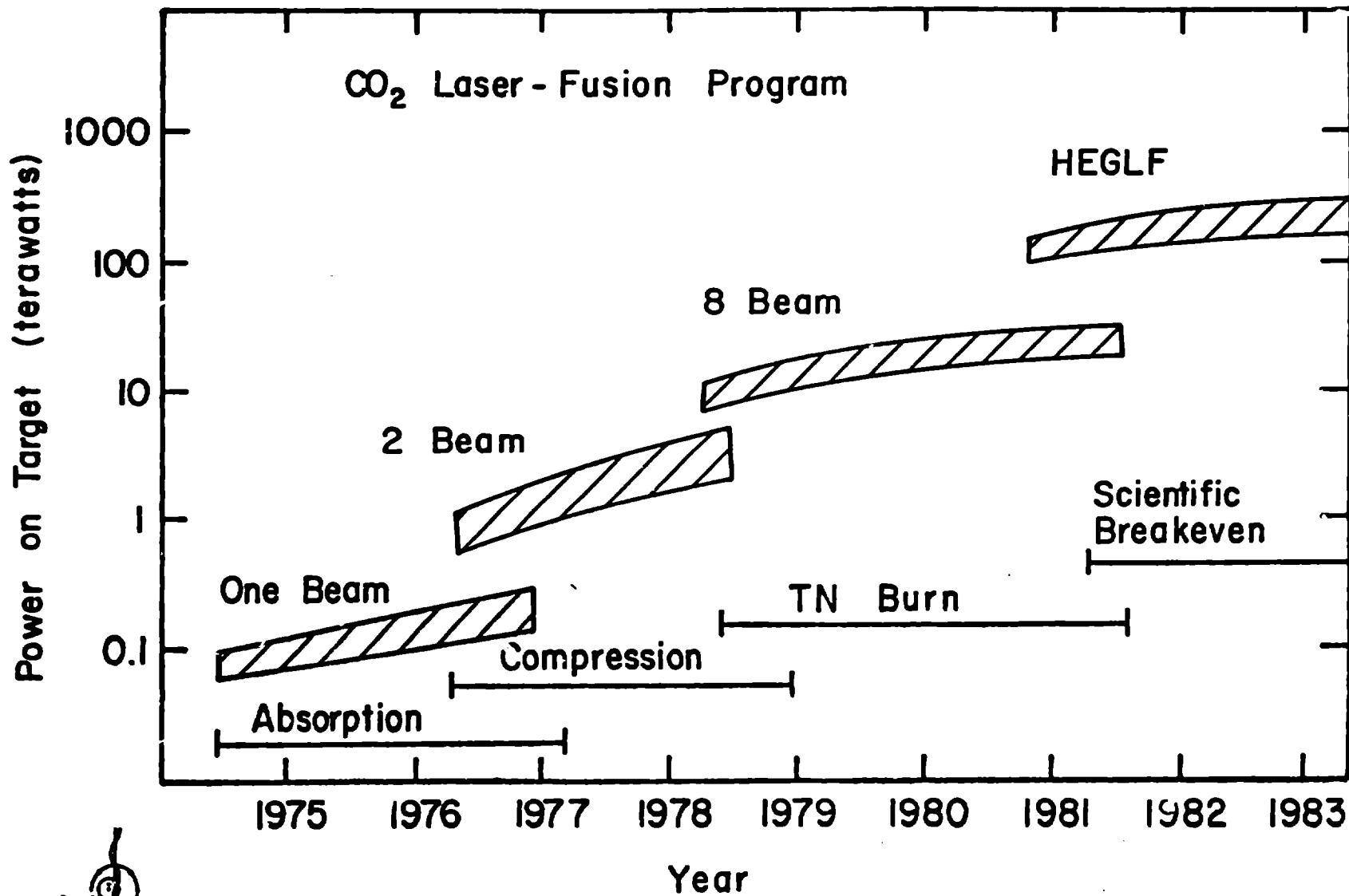
SLIDE 7

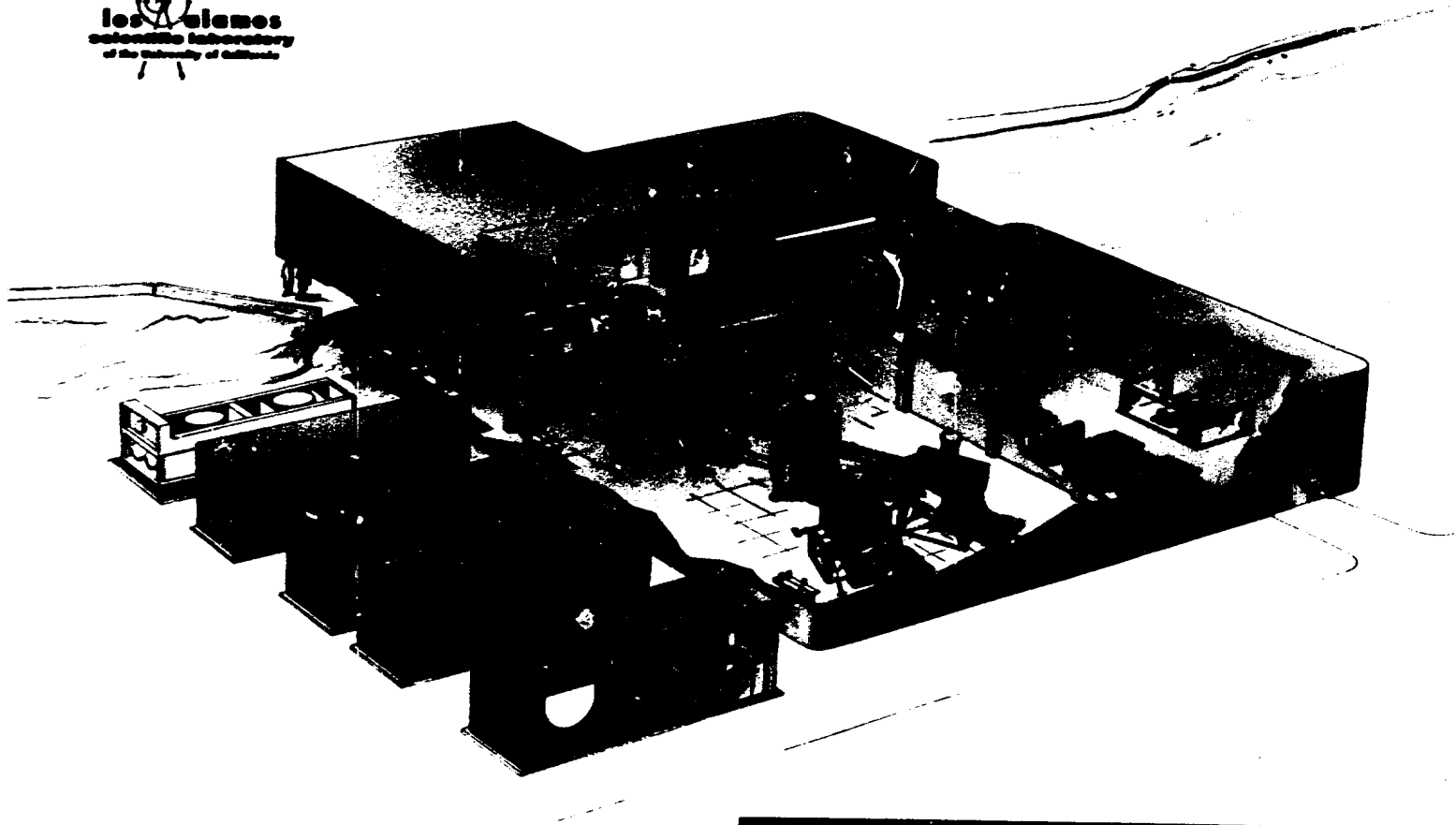


DUAL BEAM MODULE CROSS-SECTION



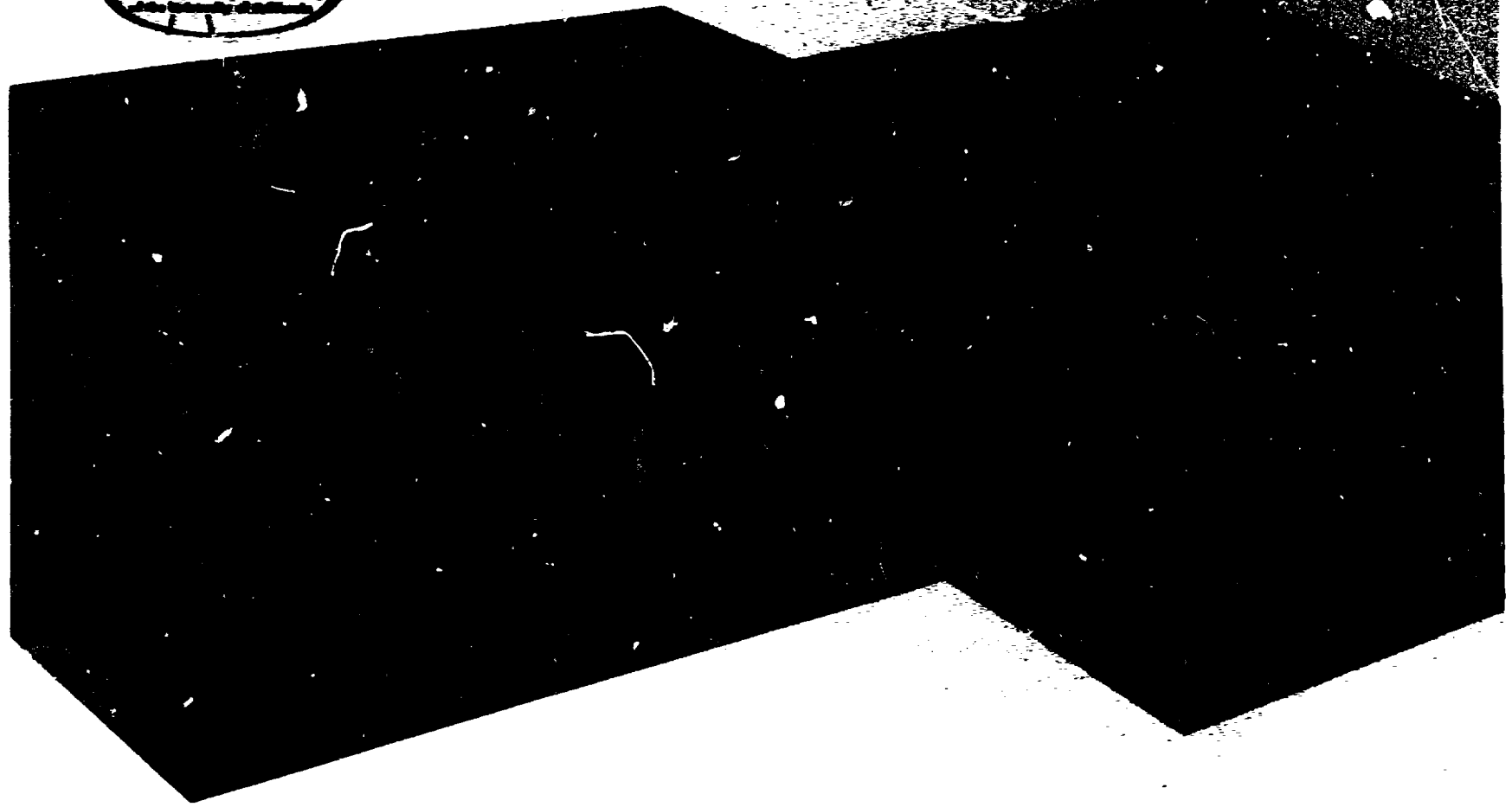


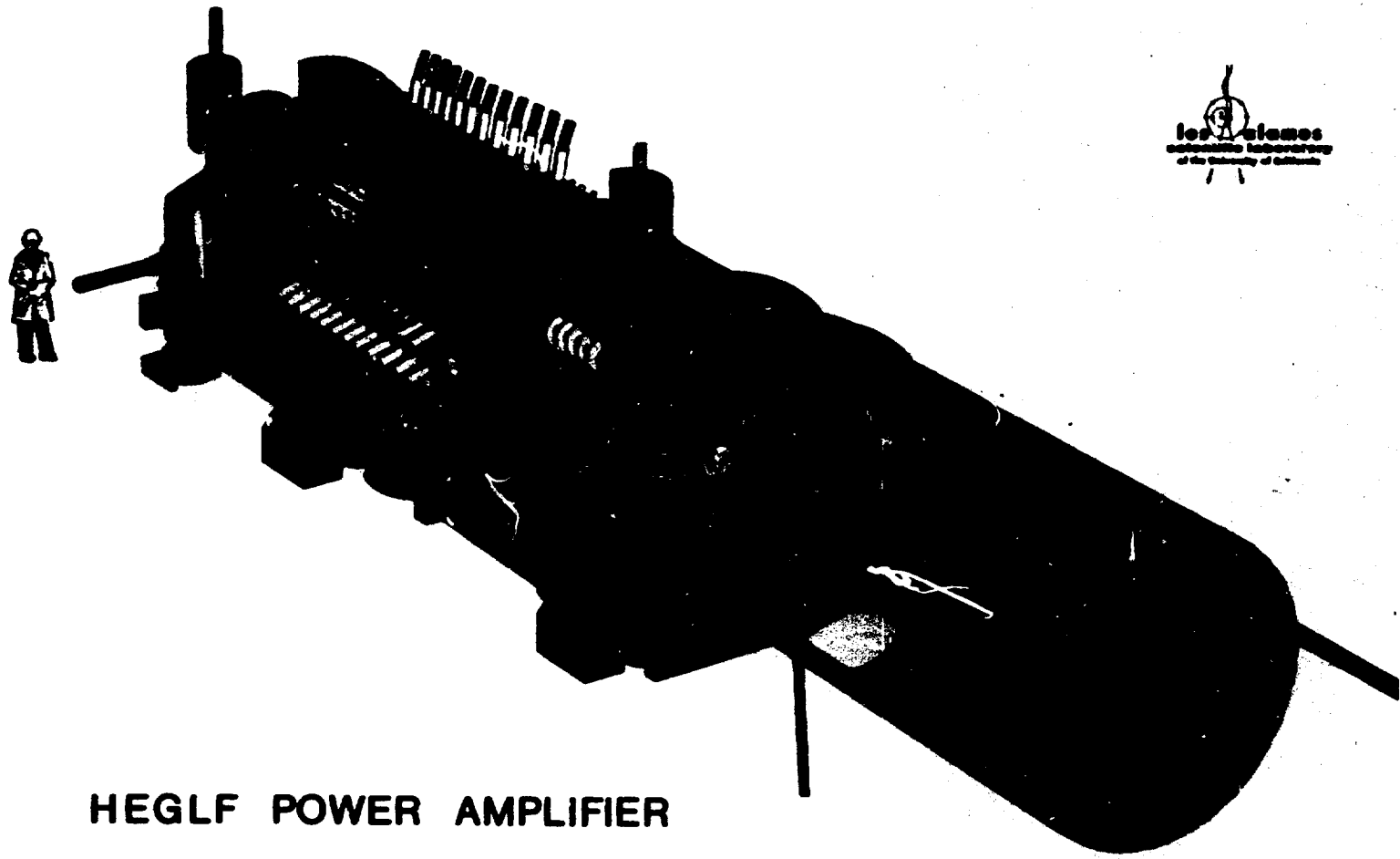




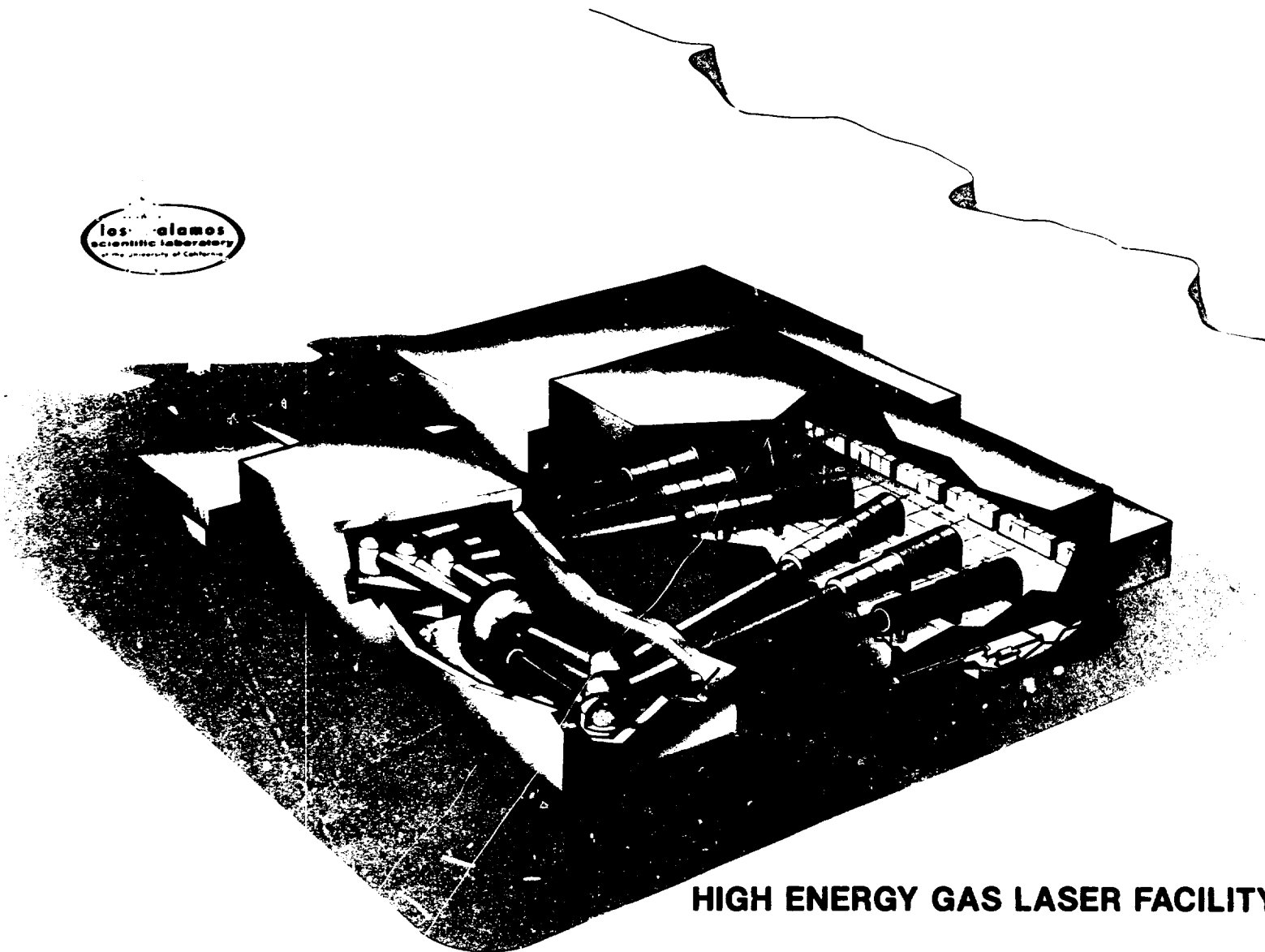
LASER FUSION LABORATORY

10 kJ 8-BEAM CO₂ LASER & TARGET CHAMBER

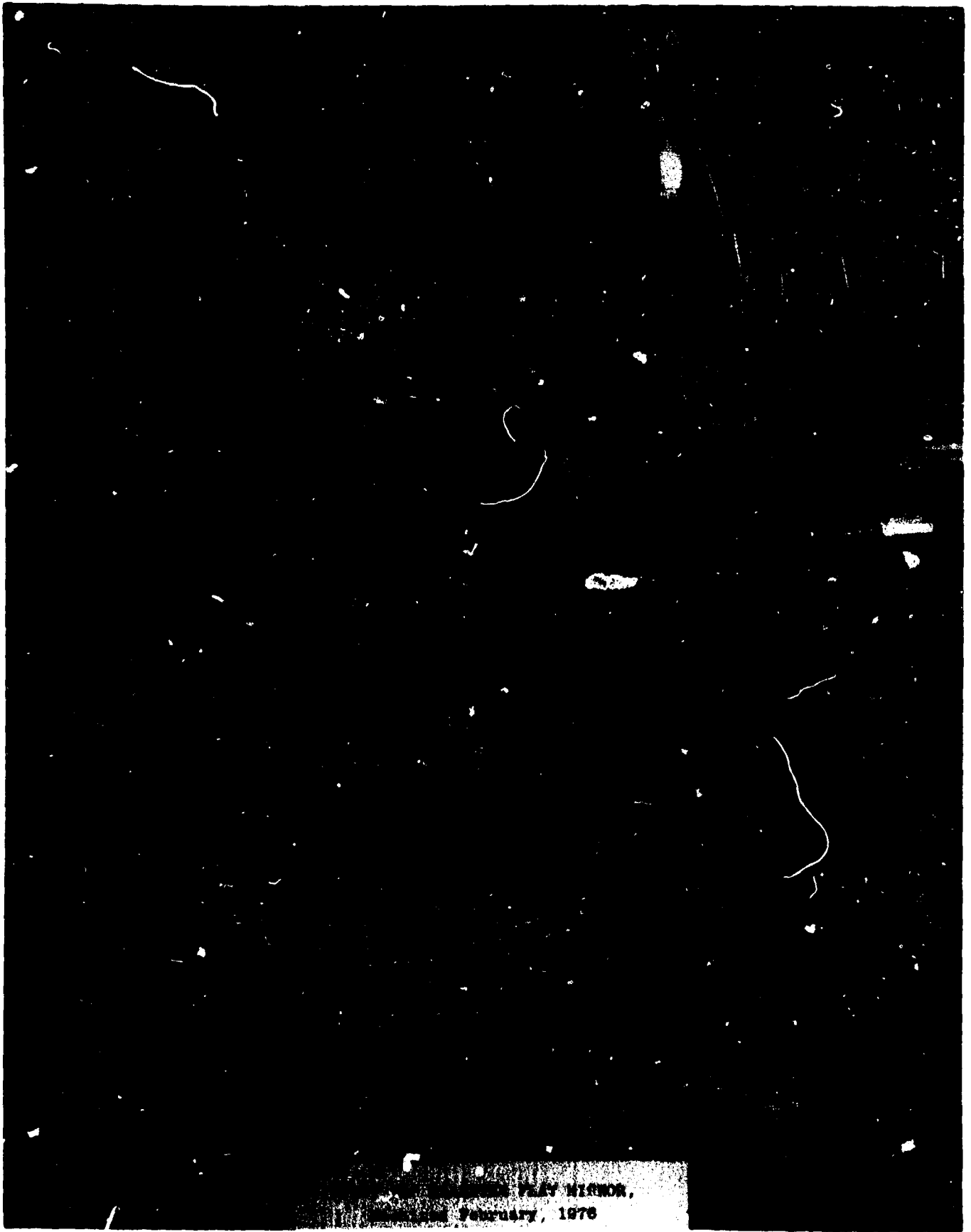




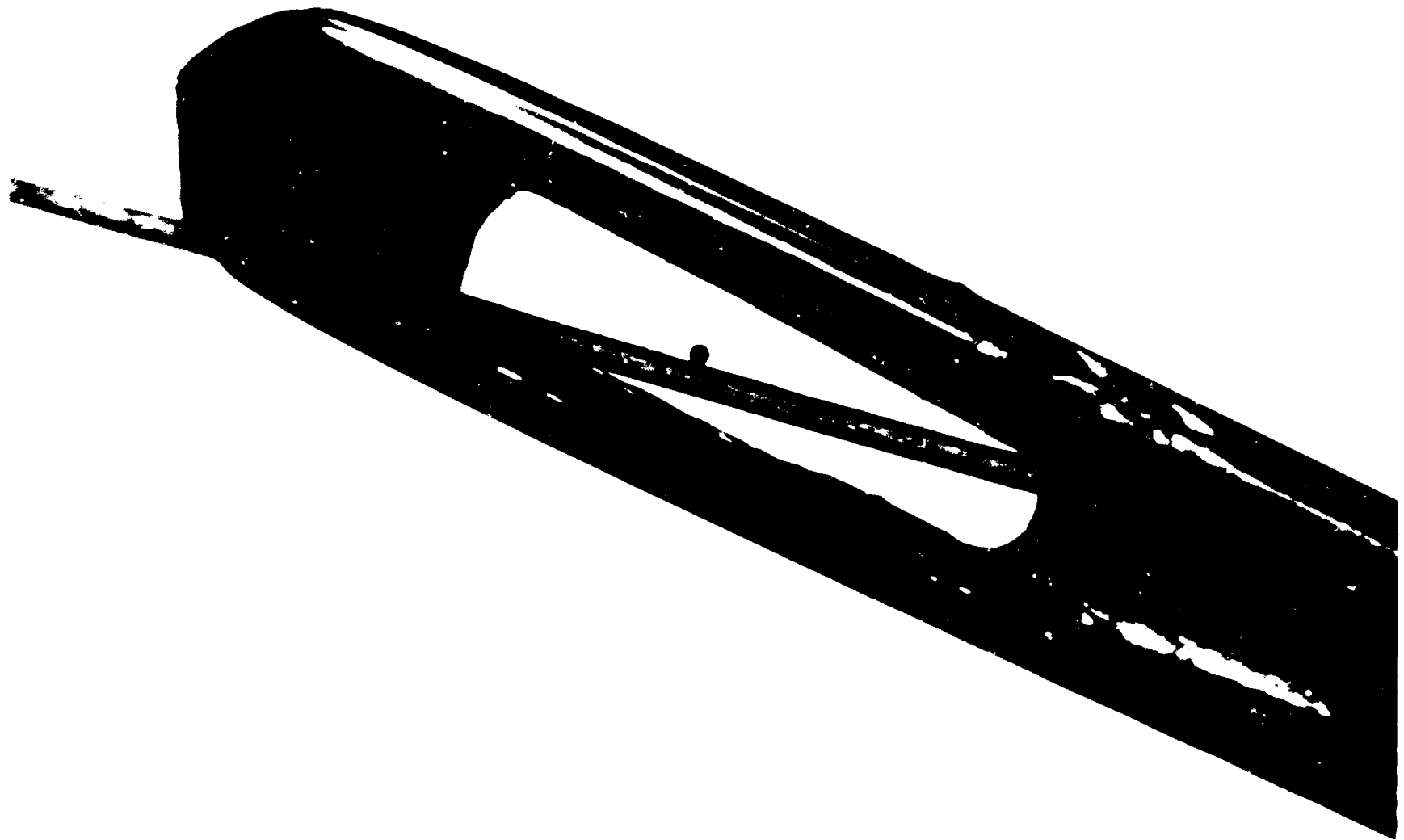
HEGLF POWER AMPLIFIER



HIGH ENERGY GAS LASER FACILITY



FRANKLIN D. ROOSEVELT
FEBRUARY, 1978

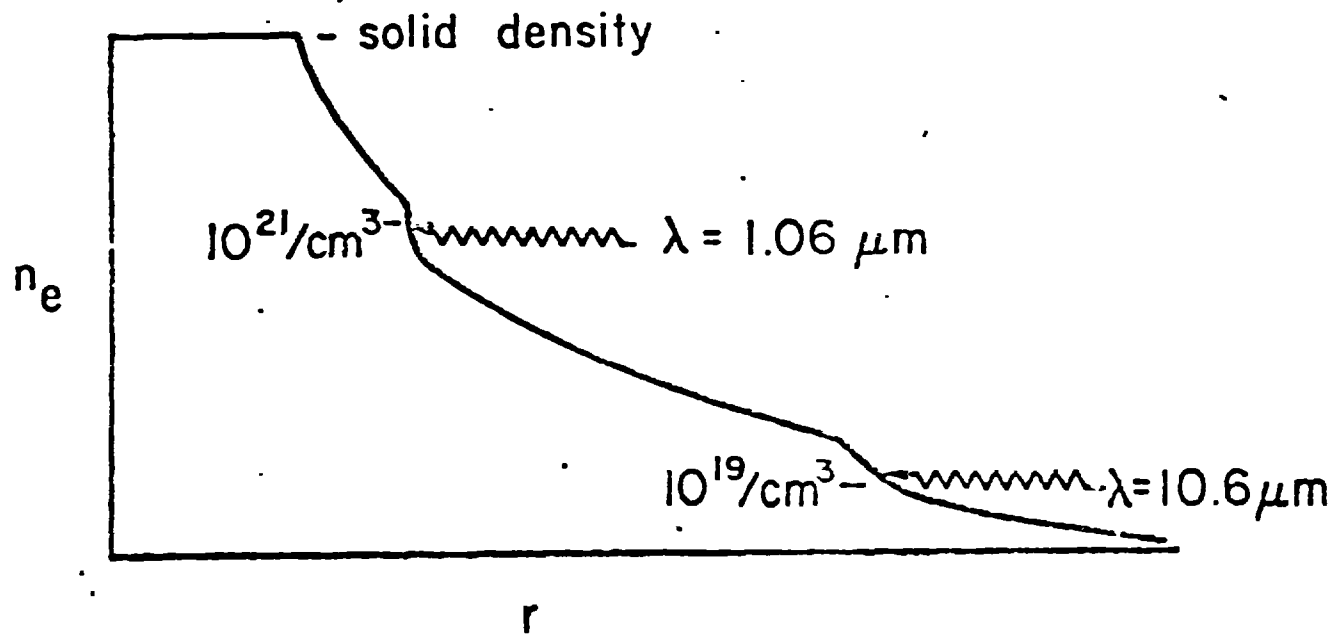


DIAGNOSTIC INSTRUMENTATION

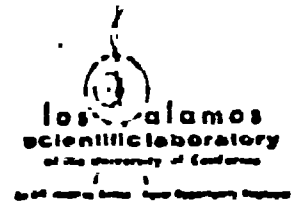
<u>DETECTOR</u>	<u>DETECTED</u>	<u>PURPOSE</u>	<u>RESOLUTION AND RANGE</u>
CALORIMETER	PHOTON, IONS	LASER AND PLASMA ENERGY MEASUREMENT	10%, μJ to 1 kJ
STREAK CAMERA	FAR-ir TO X-RAY PHOTONS	COMPRESSION AND LASER TIME HISTORY	1 ps, 20 $\mu\text{p/mm}$, 20 μm to 10 keV
PHOTO-DETECTORS	PHOTONS	LASER TIME PROFILE	30 ps, 0.1 to 10 μm
PINHOLE CAMERA	X-RAY	COMPRESSION, ALIGNMENT, TEMPERATURE	5 μm , 1 to 5 keV
X-RAY MICROSCOPE	X-RAY	COMPRESSION, DENSITY TEMPERATURE	2 μm , 0.2 to 5 keV
SPECTROMETER (PHOTON)	X-RAY LINES AND CONTINUUM	ELECTRON TEMPERATURE	0.002 \AA , 0.5 to 5 keV (lines)
MASS SPECTROMETER	ION, ELECTRONS	ENERGY BALANCE, ABSORPTION, TEMPERATURE	10%, 0.1 to 200 keV (continuum)
FILM	X-RAY, VISIBLE, ir	IMAGING AND SPECTROSCOPY	$\Delta Z = \pm 1$, $\Delta E = 10\%$

DIAGNOSTIC INSTRUMENTATION
(CONTINUED)

<u>DETECTOR</u>	<u>DETECTED</u>	<u>PURPOSE</u>	<u>RESOLUTION AND RANGE</u>
NUCLEAR TRACK DETECTORS	IONS	SPECTROMETER DETECTOR PARTICLE IMAGING	Z = 1, 92E = 10 keV to 10 MeV
CHARGED PARTICLE TRANSPORT SYSTEMS	IONS, ELECTRONS	IMAGING FOR ENERGY DISTRIBUTION	20 μm , $\pm 10\%$ energy 10 keV to 10 MeV
TV SYSTEMS	PHOTONS	ALIGNMENT, SPECTROSCOPY	0.1 to 10 μm , 10 lp/mm
INTERFEROMETERS	PHOTONS (2- λ)	PLASMA DENSITY PROFILE	5 ps, 3 μm
SCINTILLATOR, PMT	n, α , p, Z	TN YIELD, TEMPERATURE ENERGY BALANCE	n = $\pm 10\%$, 3 ns, ($I_{\text{PMT}} = 1 \text{ amp}$)
ACTIVATION COUNTER	n	TN YIELD	n = $\pm 10\%$, limited energy range
FARADAY CUPS	Z	ENERGY BALANCE	n = $\pm 10\%$, 1 ns



SLIDE 21



10/6/76

$$\frac{P_{\text{LASER}}}{P_{\text{KINETIC}}} = \frac{E_0^2}{8\pi} \frac{1}{n_{\text{cr}} T} = 2.1 \times 10^{-16} \frac{\Phi_L \lambda^2}{T}$$

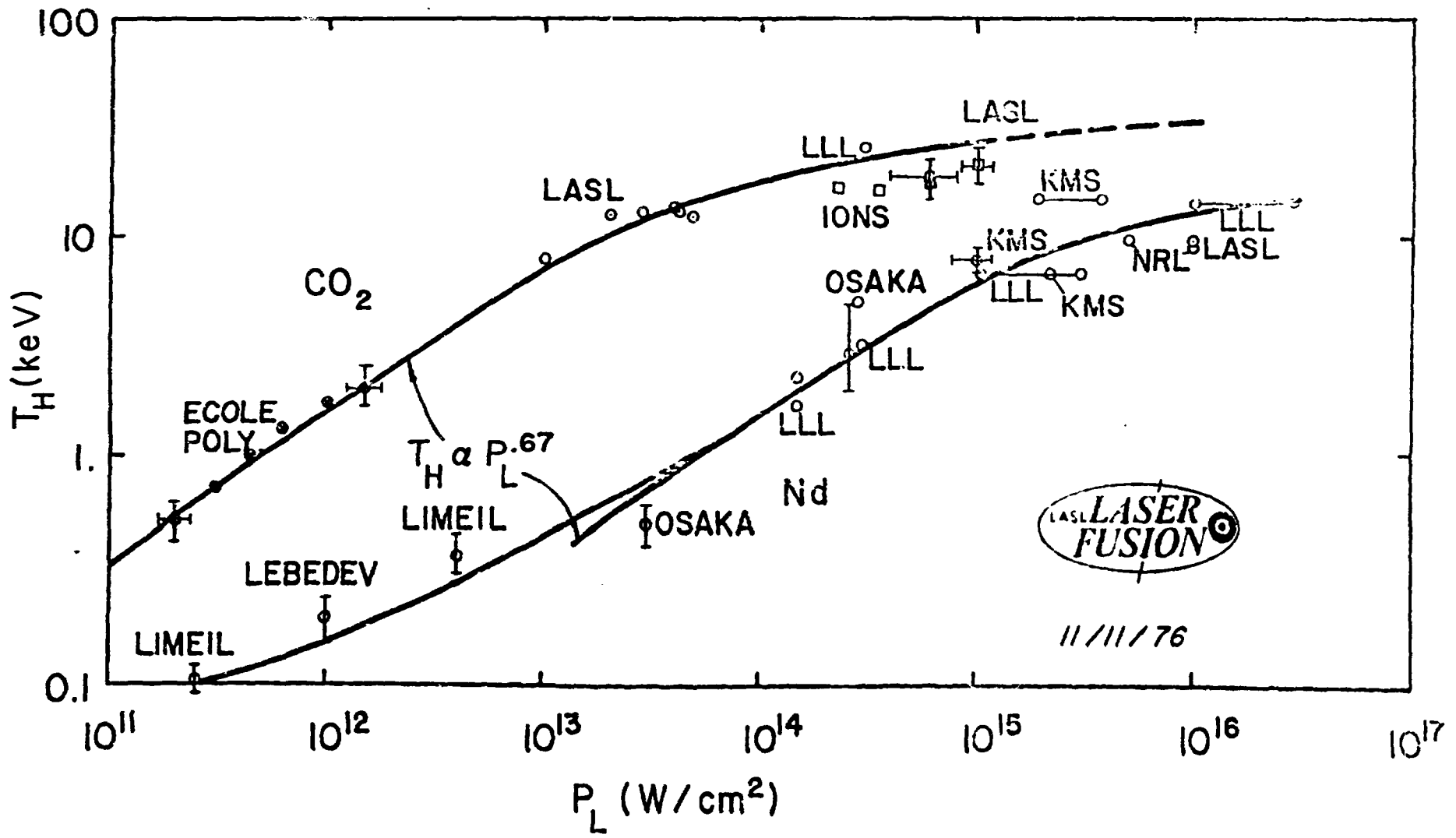
T in keV, Φ_L in W/cm², λ in μm

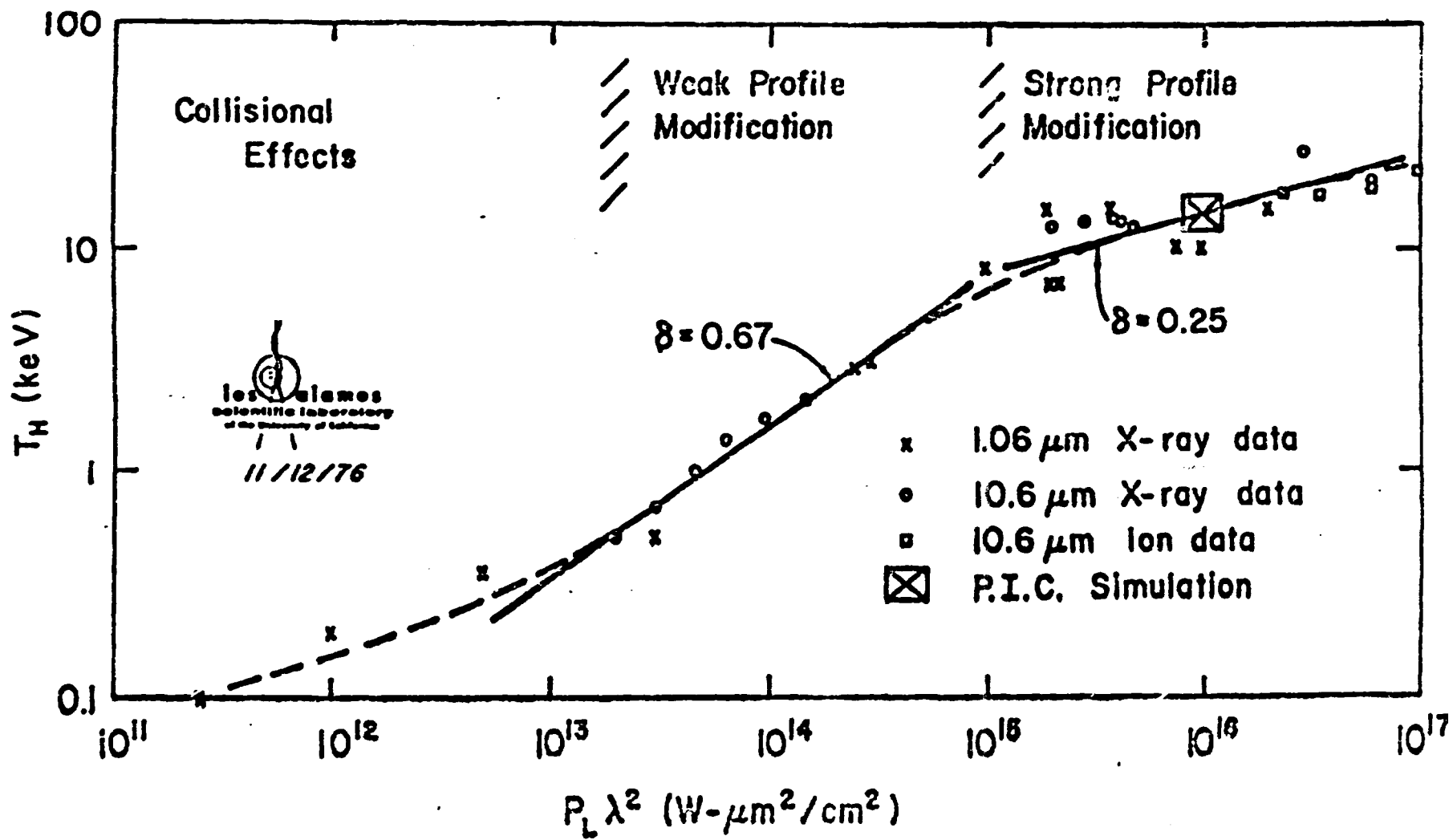
For $\Phi_L = 10^{15}$ W/cm², T = 1 keV:

$$\frac{P_{\text{LASER}}}{P_{\text{KINETIC}}} = \begin{cases} 0.2 \text{ for Nd} \\ 20 \text{ for CO}_2 \end{cases}$$

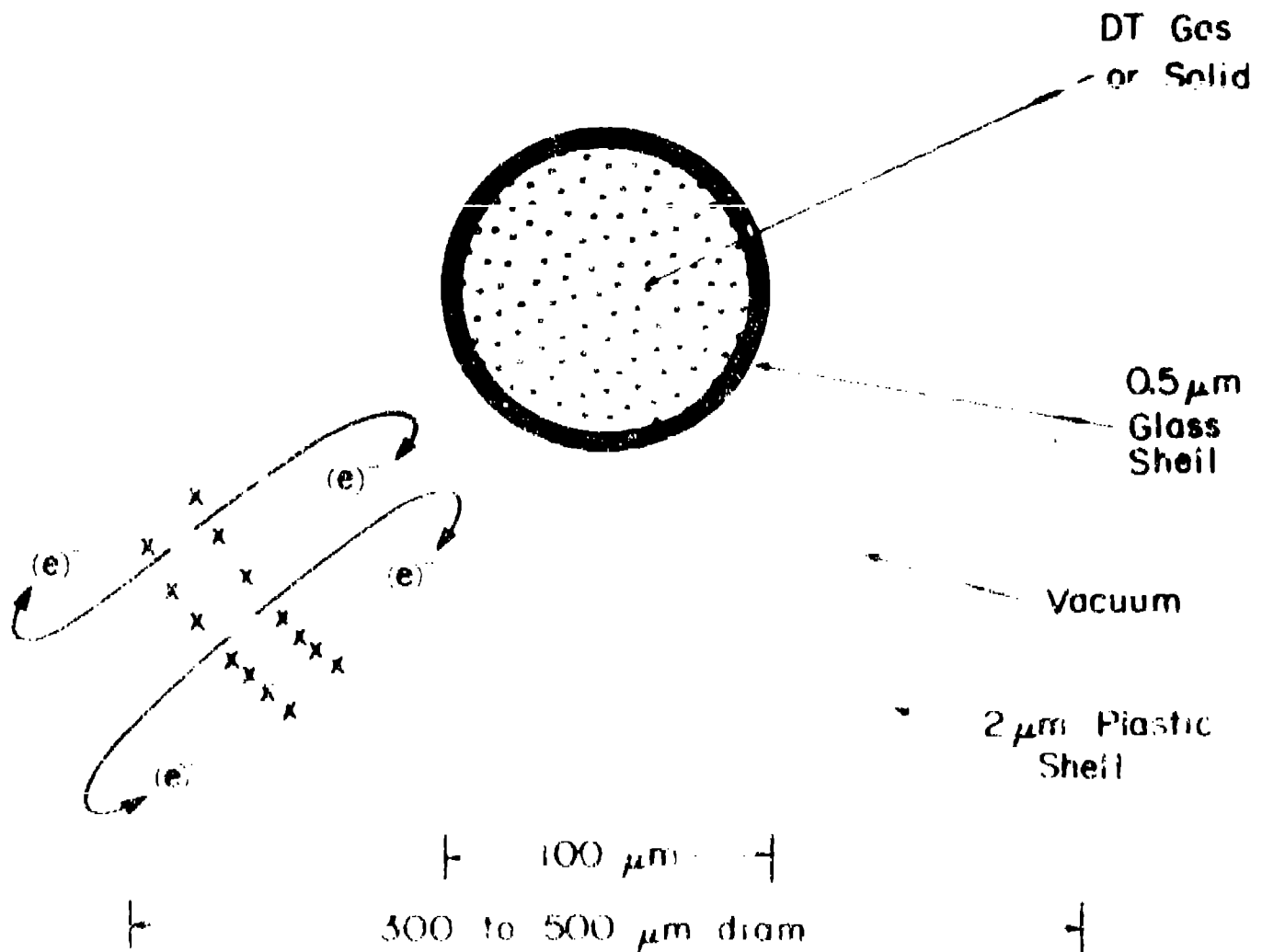


10/7/76

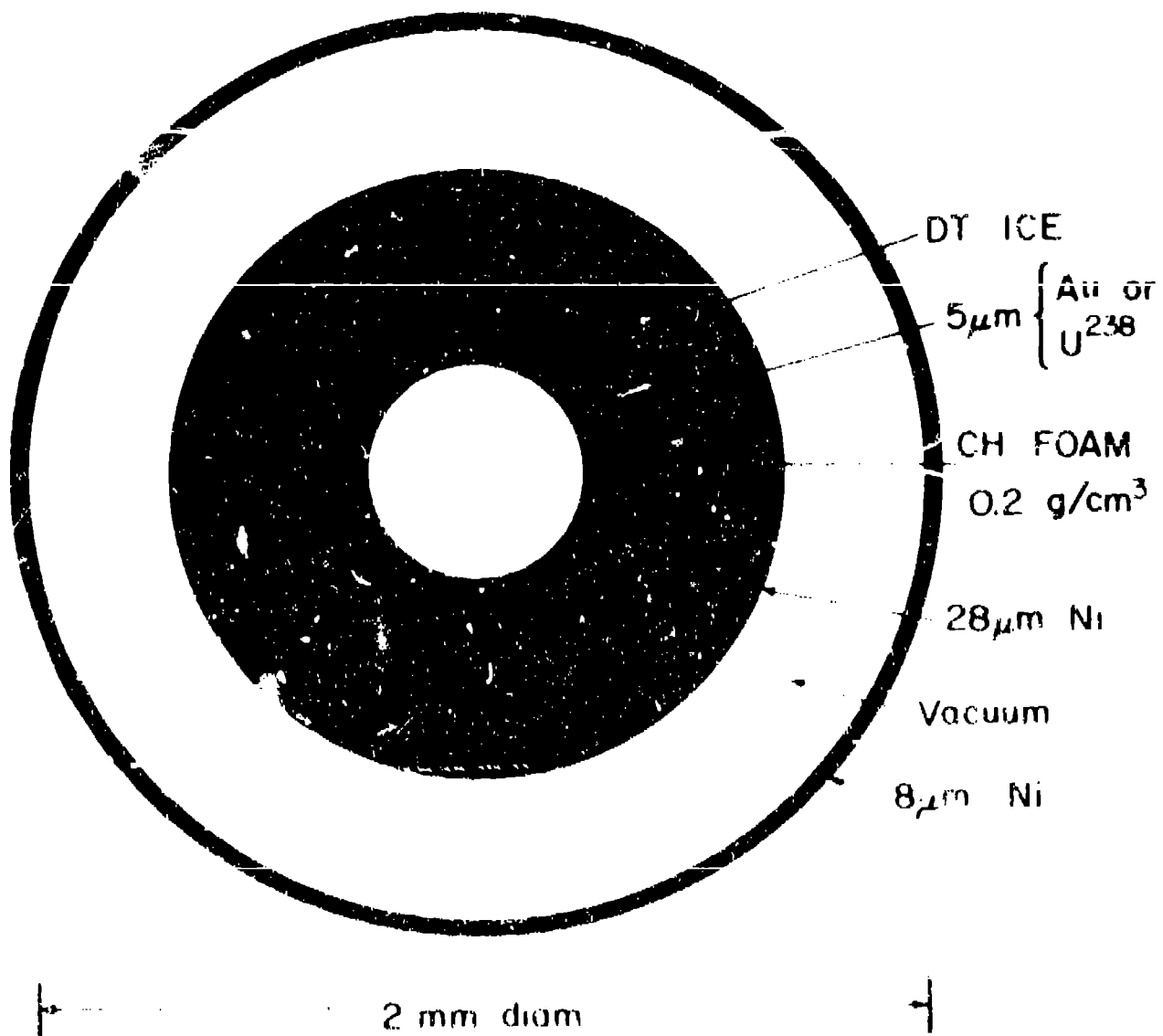




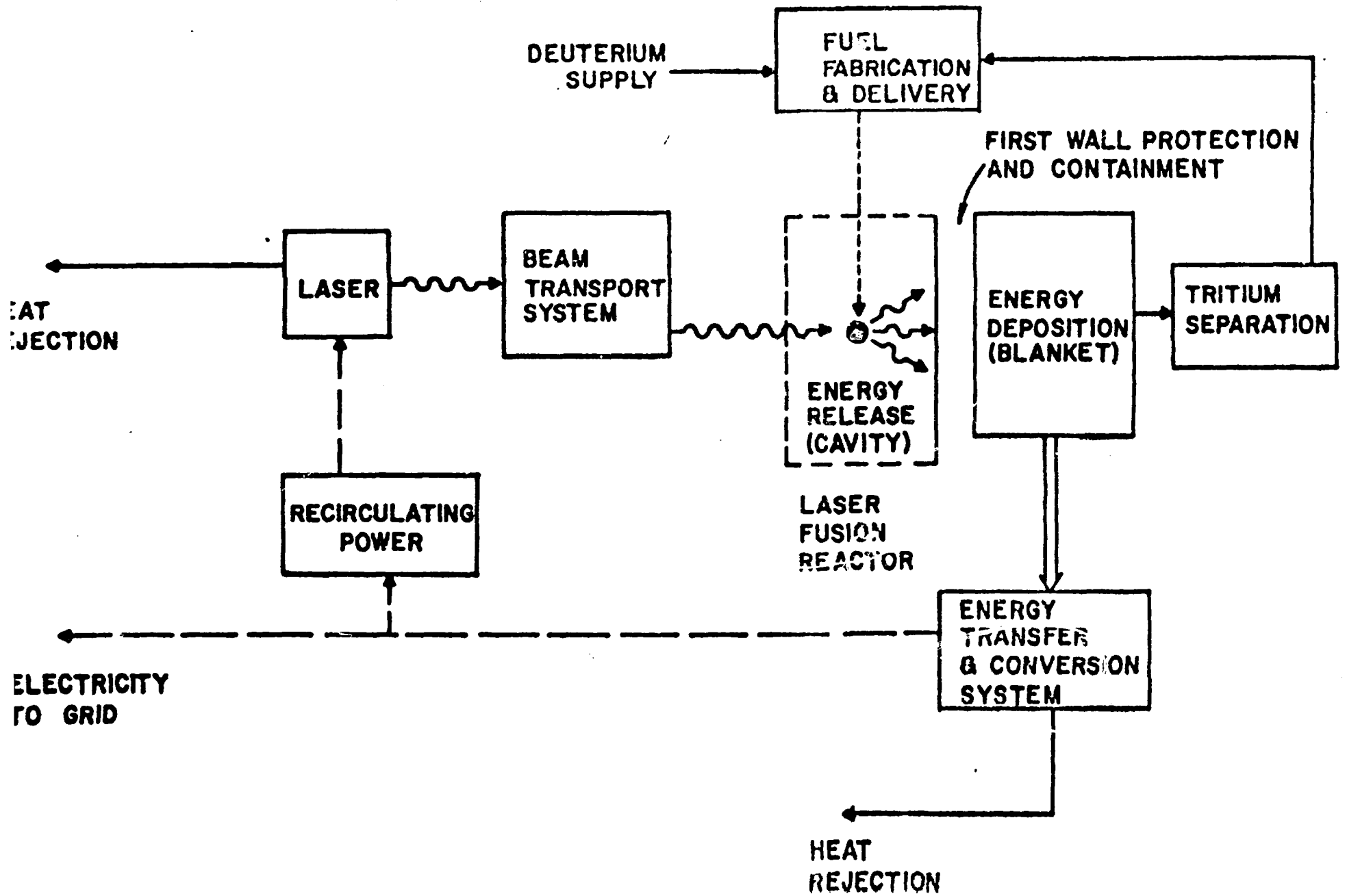
SLIDE 24



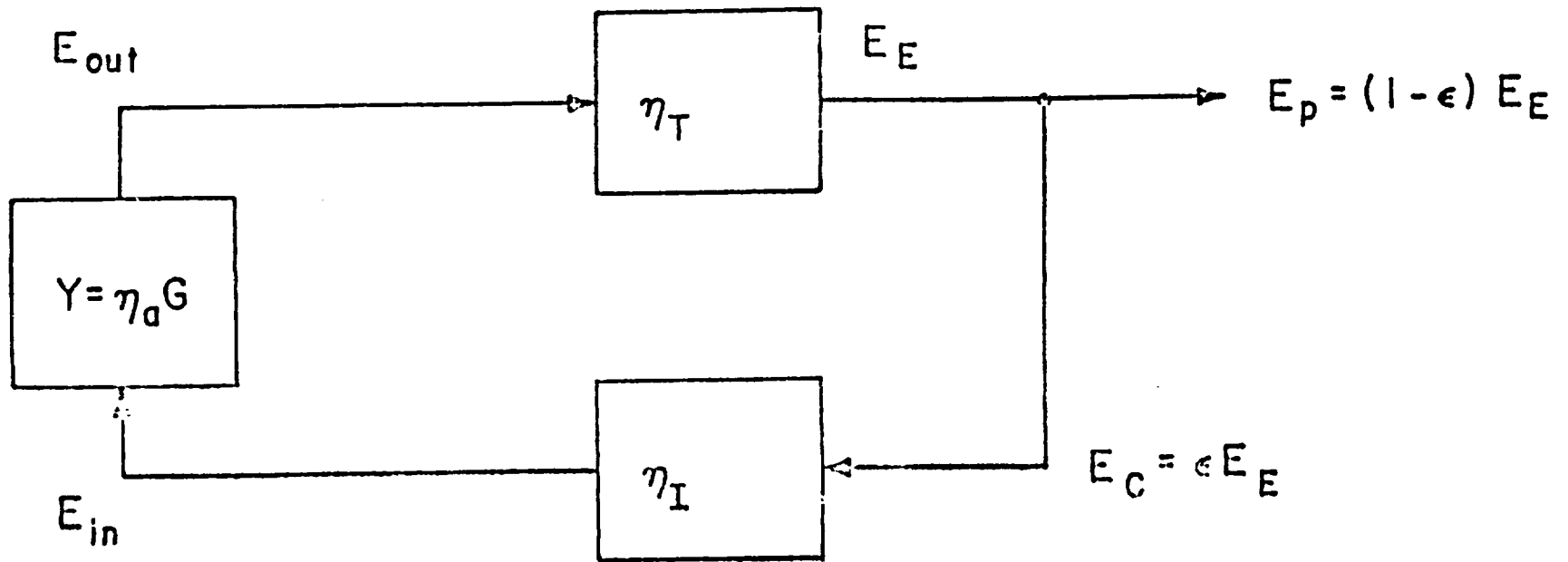
Vacuum Insulation Target



Multi Shell Laser Target



ENERGY FLOW DIAGRAM



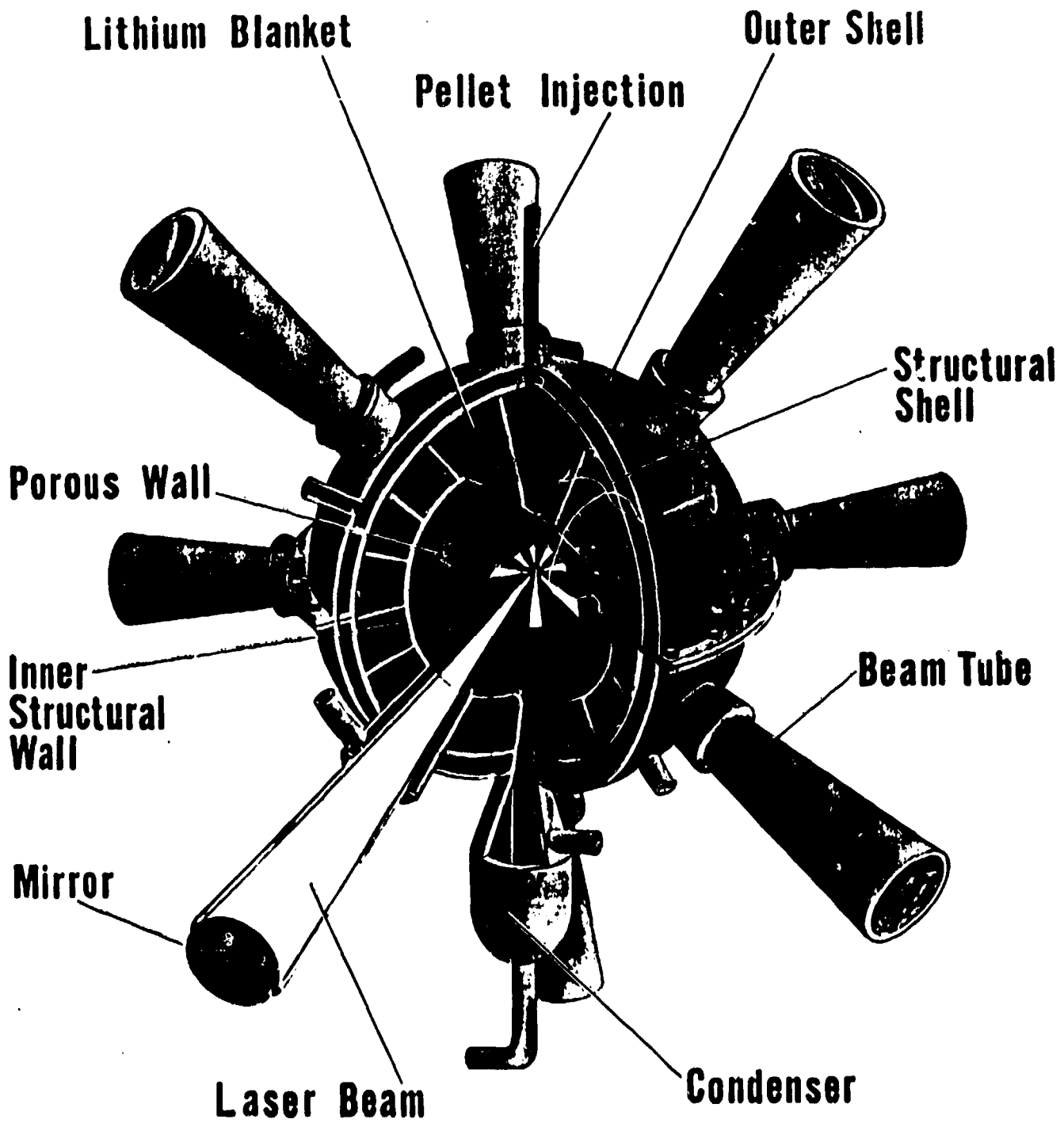
$$\epsilon = (\eta_I Y \eta_T)^{-1}$$

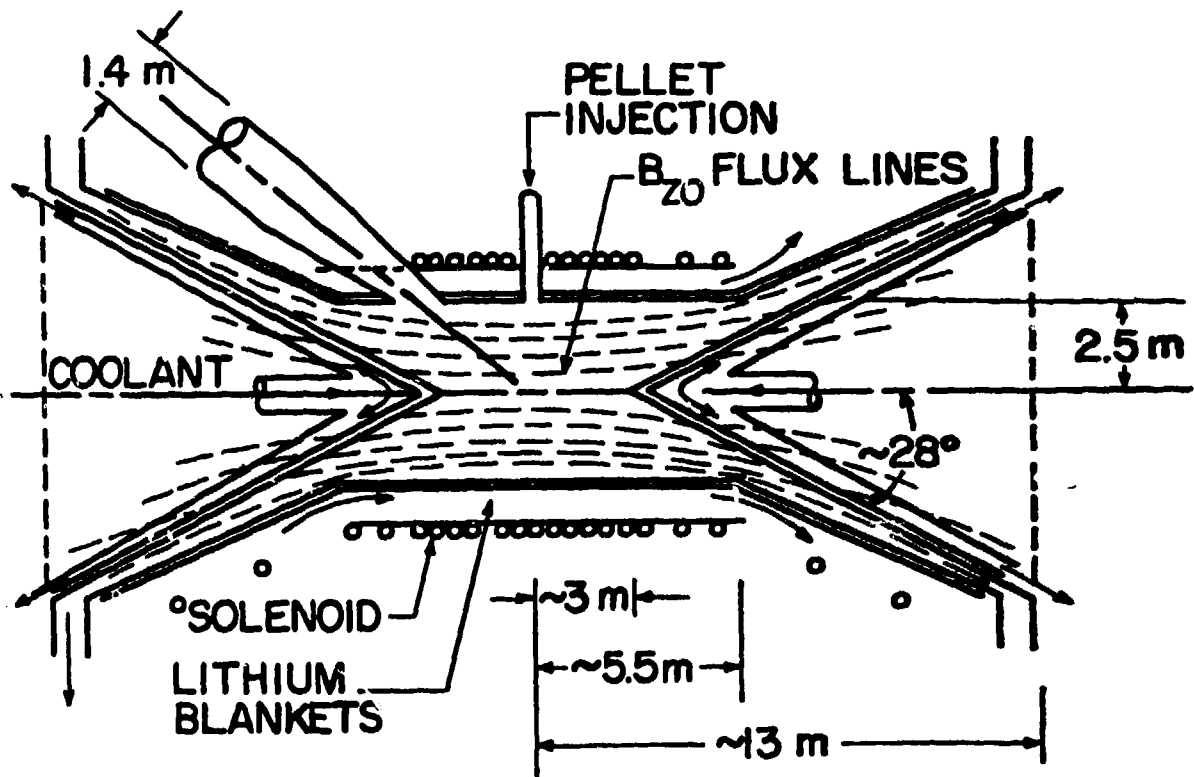
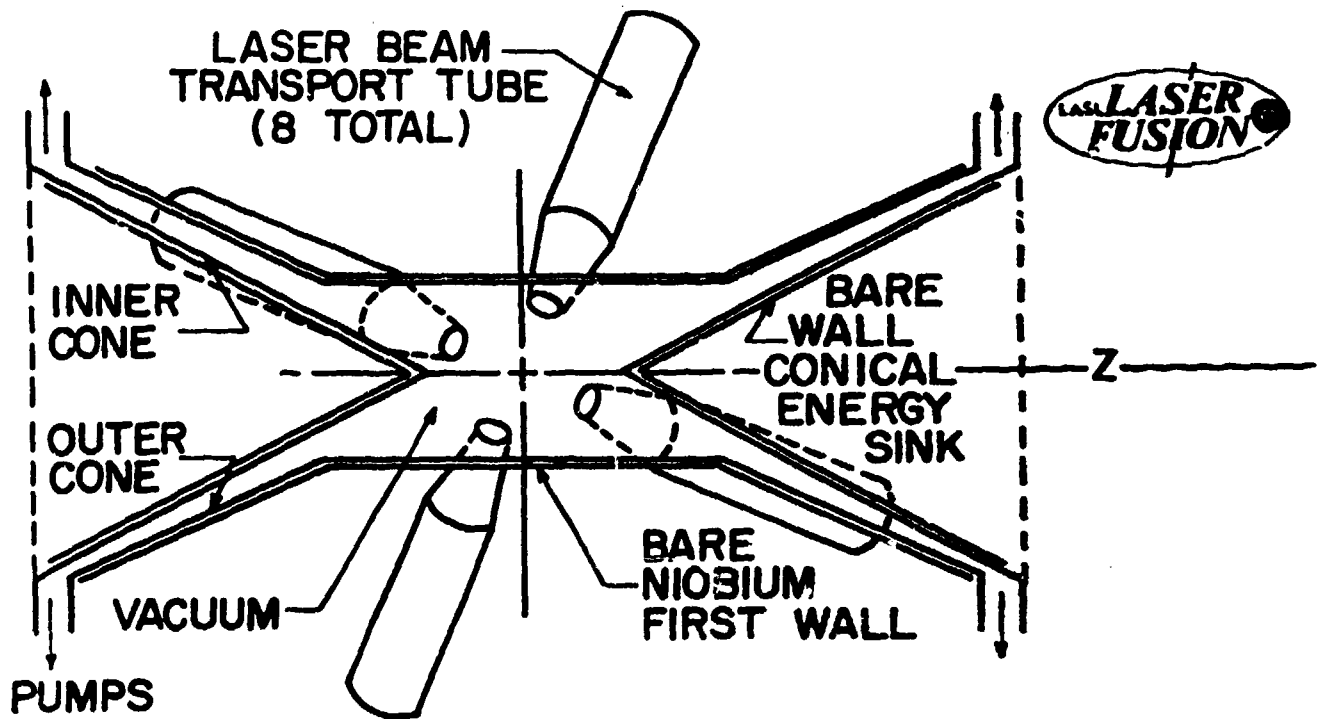
$$G > (\epsilon \eta_T \eta_a \eta_I)^{-1}$$

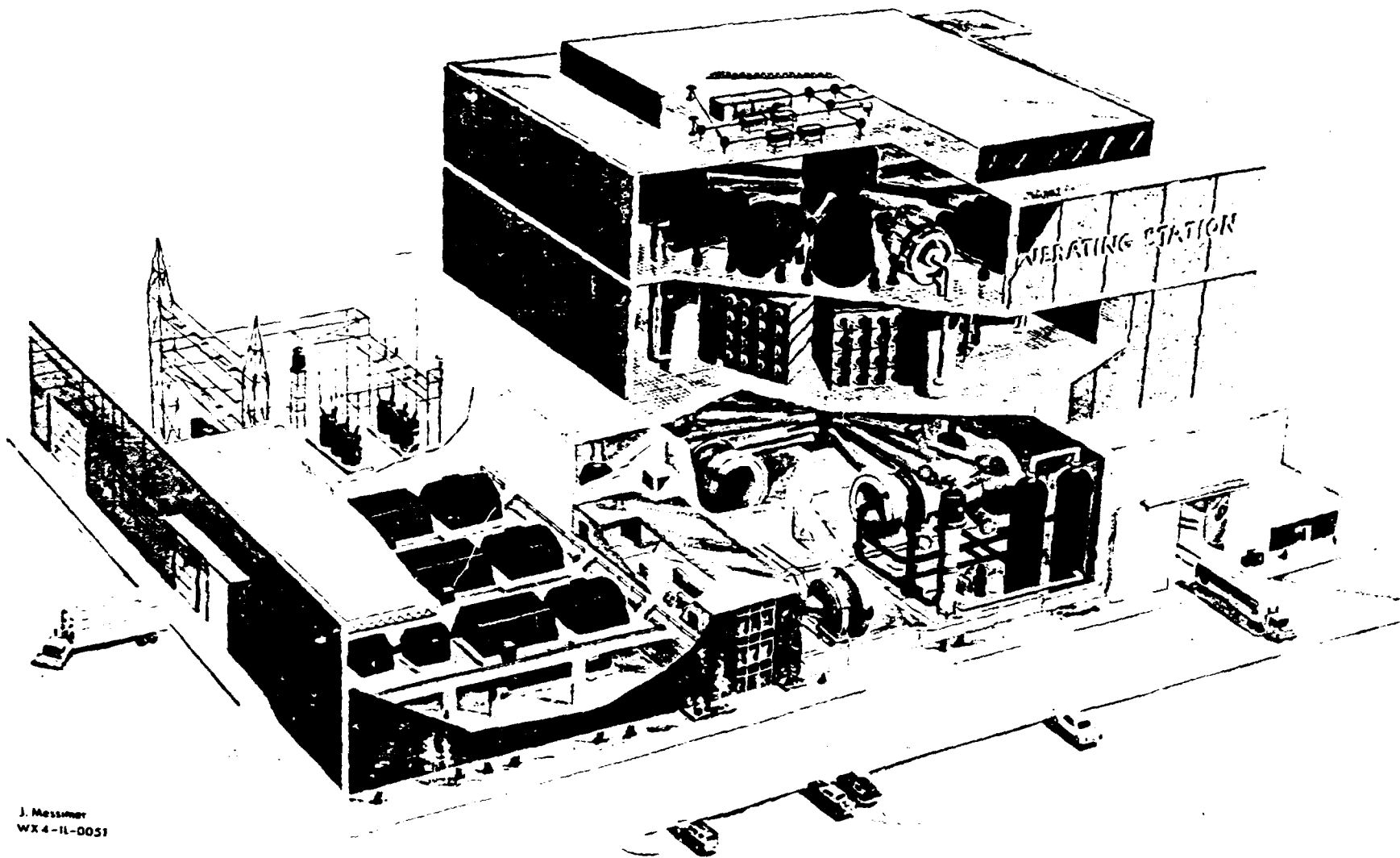
$$> (.3 \times .35 \times .3 \times .05)^{-1} = 635$$



1/27/77

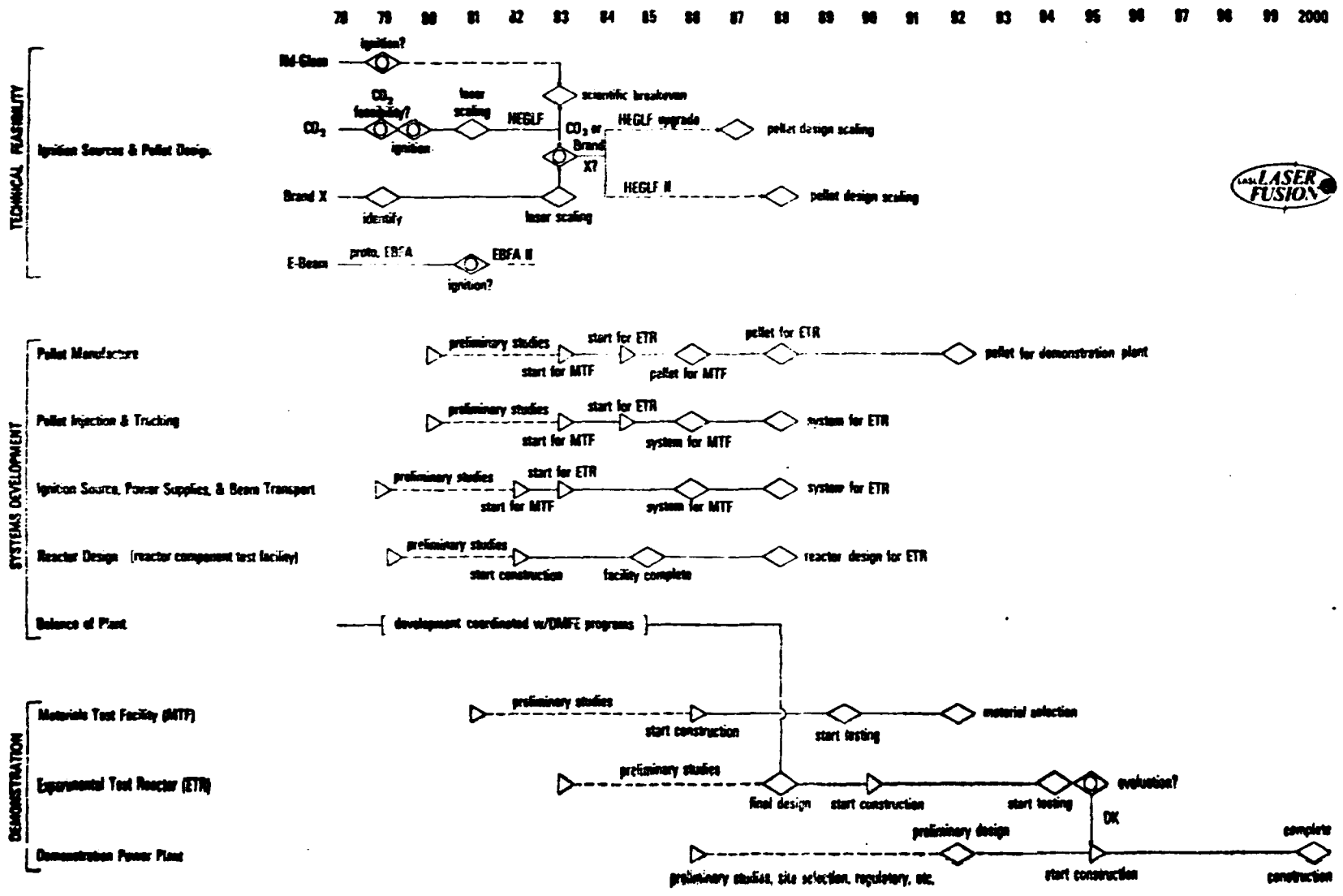






J. Messmer
WX 4-IL-0051

CONCEPTUAL 1170 MW(e) LFR GENERATING STATION



SLIDE 32